Effects of space weather on the Earth's ionosphere

Operational Space Weather Fundamentals

L'Aquila, 13-17 May, 2024

Kirsti Kauristie, Finnish Meteorological Institute

FMI

Contents

- Brief introduction on radiowave propagation in the ionosphere
- Examples of space weather effects - waves in the MHz range
  - The case of signal attenuation: D-layer absorption
  - The case of signal loss: Dilute ionosphere
- Examples of space weather effects - waves in GHz range
  - Brief intro to Global Navigation Satellite Systems
  - The case of signal diffraction: Ionospheric scintillation
  - The case of signal dispersion: Ionospheric delay
- Examples of ionospheric products in space weather services
- Summary

Factors controlling ionospheric electron density & Ionospheric impact on radio waves

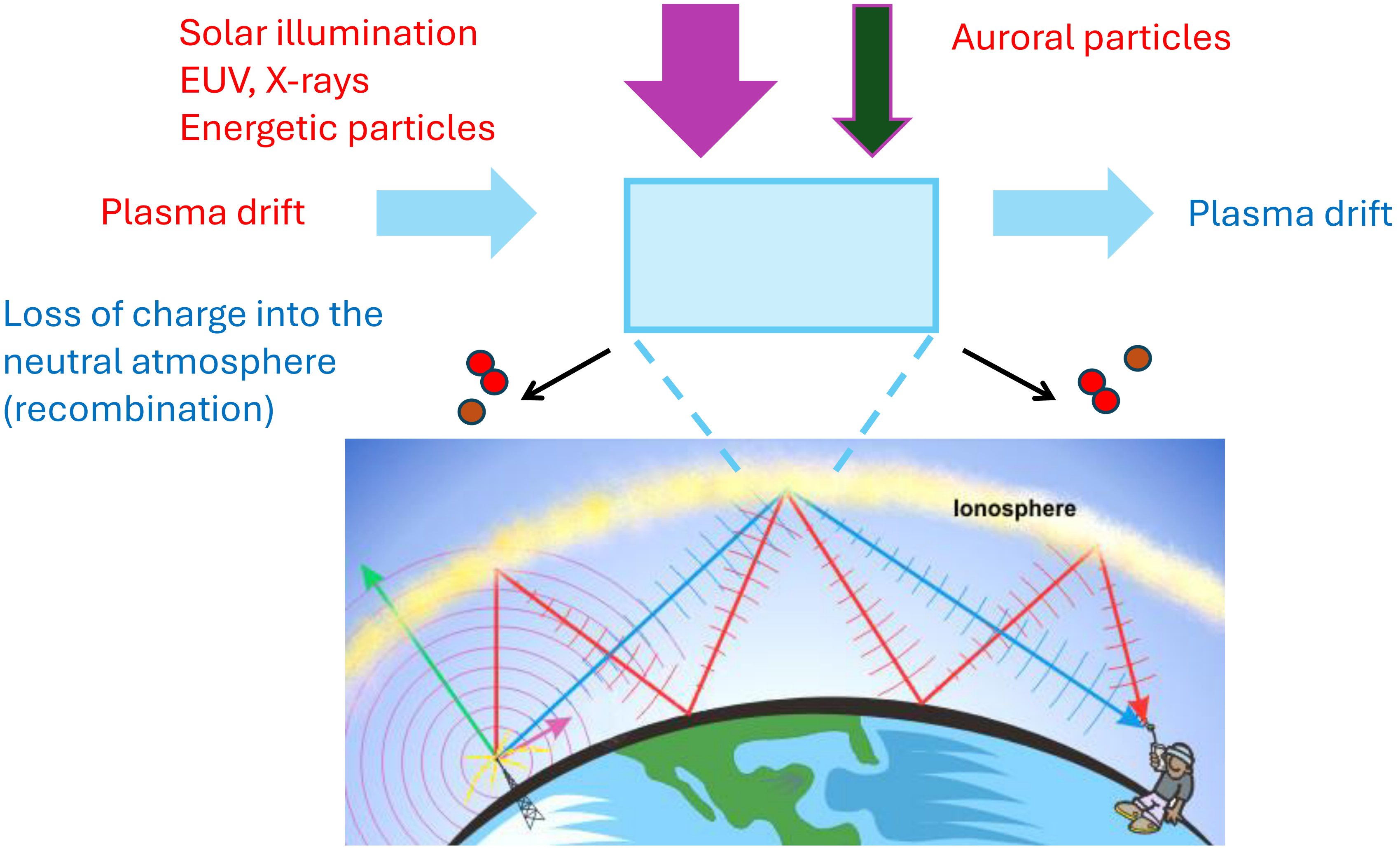

Ionospheric impacts Radio waves:

- Refraction
- Dispersion (velocity depends on frequency)
- Diffraction in wave fronts -> scintillation
- Scattering (coherent and incoherent)
- Polarization changes
- Attenuation

More about refraction

- Characterized with refraction index n, depends
  - On the frequency (f) of the radio wave, $\omega=2\pi f$
  - On background conditions

- Is linked with the group and phase velocity of the wave
  - Phase velocity $v_p=\lambda f=\omega/k$ & $v_p=c/n(\omega)$
  - Group velocity $v_g=d\omega/dk=c/(n(\omega)+\omega\frac{dn(\omega)}{d\omega})$

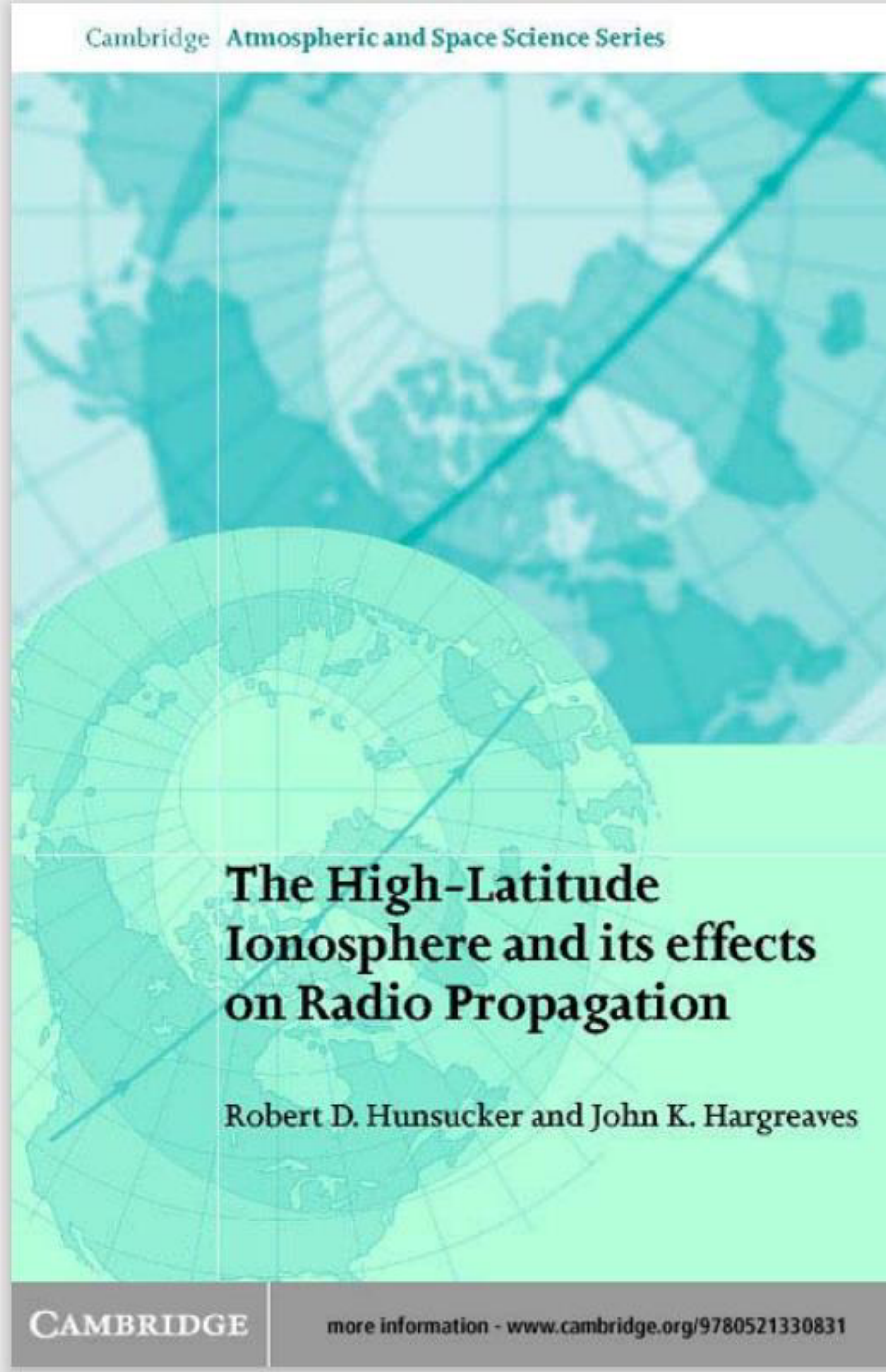

Refraction index in ionized media: Appleton-Hartree equation

$$n^2 = 1 - \frac{X}{1 - jZ - \frac{Y_T^2}{2(1 - X - jZ)} \pm \left(\frac{Y_T^4}{4(1 - X - jZ)^2} + Y_L^2 \right)^{1/2}}$$

$$j = \sqrt{-1}$$

Plasma frequency

$$\omega_N = [Ne^2/\varepsilon_0 m_e]^{1/2}$$

Gyrofrequency

$$\omega_B = Be/m_e,$$

$$X = \omega_N^2/\omega^2,$$

$$Y = \omega_B/\omega,$$

$$Z = \nu/\omega.$$

$$Y_L = Y\cos\theta$$

$$Y_T = Y\sin\theta,$$

N= electron density
e= electron charge
m_e=electron mass
ε_0= vacuum permittivity
B=magnetic field
ω=2πf, f=wave frequency
ν= electron collision rate with other particles
θ= angle between B and wave propagation direction

Appleton-Hartree equation: no collisions, no B-field

$$n^2 = 1 - \frac{X}{1 - \cancel{\mathrm{j}Z} - \cancel{\dfrac{Y_{\mathrm{T}}^2}{2(1 - X - \mathrm{j}Z)}} \cancel{\pm \left(\dfrac{Y_{\mathrm{T}}^4}{4(1 - X - \mathrm{j}Z)^2} + Y_{\mathrm{L}}^2 \right)^{1/2}}}$$

$$n^2 = 1 - \mathrm{X} = 1 - \omega_N^2/\omega^2$$

$$= 1 - Ne^2/(\varepsilon_0 m_e \omega^2).$$

$v_p=\omega/k=c/n(\omega)$ (phase velocity)
$v_g=d\omega/dk=cn(\omega)$ (group velocity)

Appleton-Hartree equation: B-field parallel to wave propogation, but no collisions

$$n^2 = 1 - \frac{X}{1 - \cancel{jZ} - \cancel{\frac{Y_T^2}{2(1 - X - jZ)}} \pm \left(\cancel{\frac{Y_T^4}{4(1 - X - jZ)^2}} + Y_L^2 \right)^{1/2}}$$

$$n^2 = 1 - X/(1 \pm Y_L)$$

$$= 1 - \omega_N^2/[\omega(\omega \pm \omega_L)$$

Splitting to ordinary and extra-ordinary polarizations

n(ω) is real → no attenuation

$\omega_L = \omega_B$

Appleton-Hartree equation: Collisions but no B-field

$$n^2 = 1 - \frac{X}{1 - jZ - \cancel{\frac{Y_T^2}{2(1-X-jZ)}} \pm \left(\cancel{\frac{Y_T^4}{4(1-X-jZ)^2} + Y_L^2} \right)^{1/2}}$$

$$n^2 = 1 - X/(1 - jZ)$$

$$= 1 - \omega_N^2/[\omega(\omega - j\nu)].$$

$$e^{-kx}$$

e-fold attenuation in distance $1/\kappa$

$$\kappa = \frac{\omega}{c}\frac{1}{2\mu}\frac{XZ}{1+Z^2}$$

$$= \frac{e^2}{2\varepsilon_0 m_e c}\frac{1}{\mu}\frac{N\nu}{\omega^2+\nu^2}.$$

Examples of space weather effects

Impacts on radio waves in MHz range

The case of attenuation: D-layer absorption

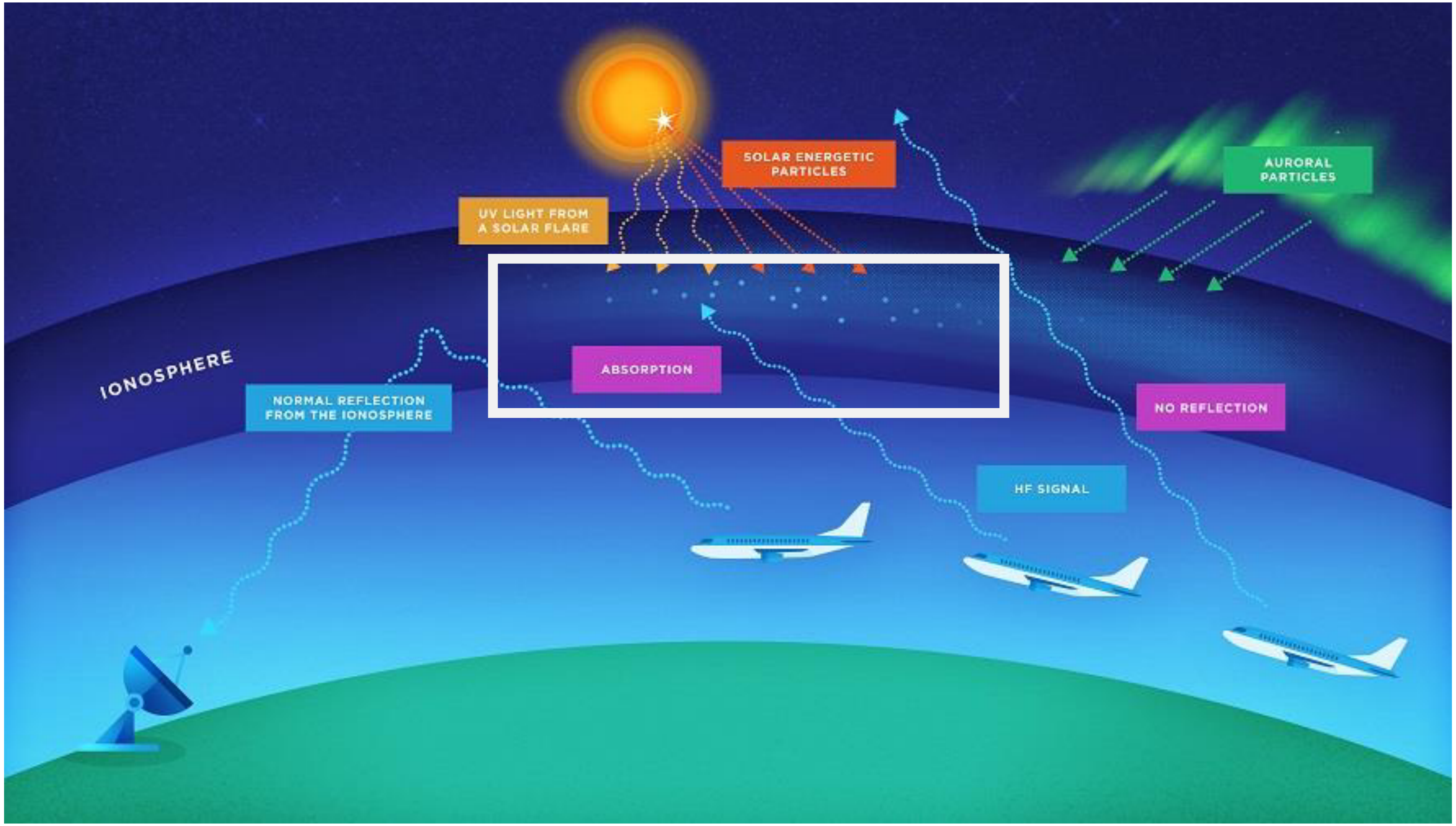

Drawing: FMI & STCE for PECASUS

D-layer absorption: causes and consequences

- **Causes:**
  - Solar bursts of X-rays: Attenuation in the dayside ionosphere
  - Solar bursts of energetic protons (SEP): Attenuation in the polar caps
  - Energetic electron precipitation driven by magnetospheric processes (substorms, wave-particle interactions): Attenuation at auroral oval latitudes

- **Impacted technologies**
  - Over the horizon communication using High Frequencies (3-30 MHz)
  - HF radars
  - Systems utilizing the ground-ionosphere waveguide

Solar energetic protons

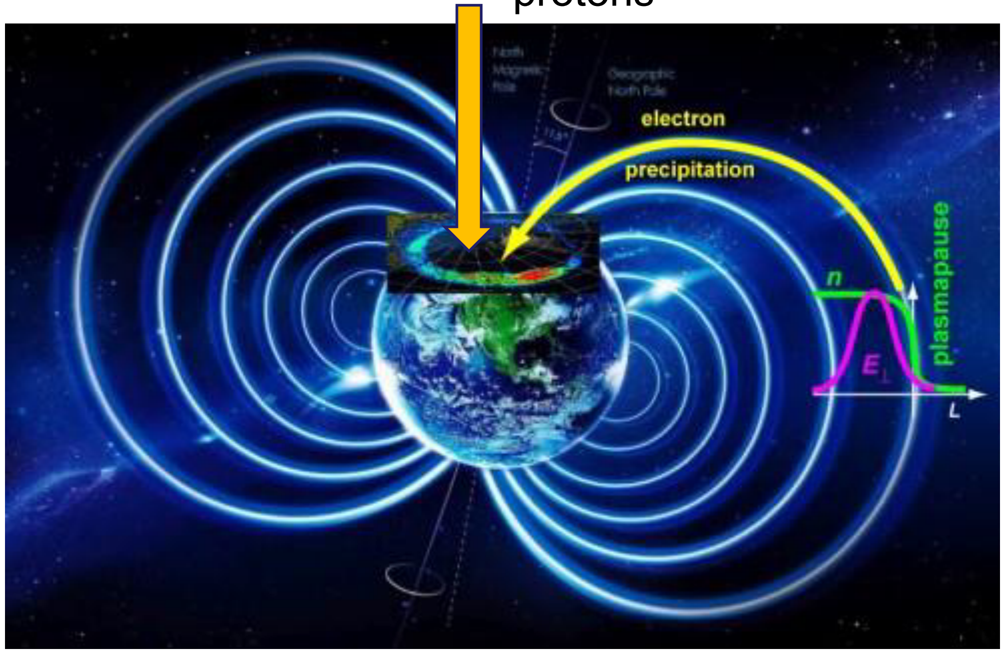

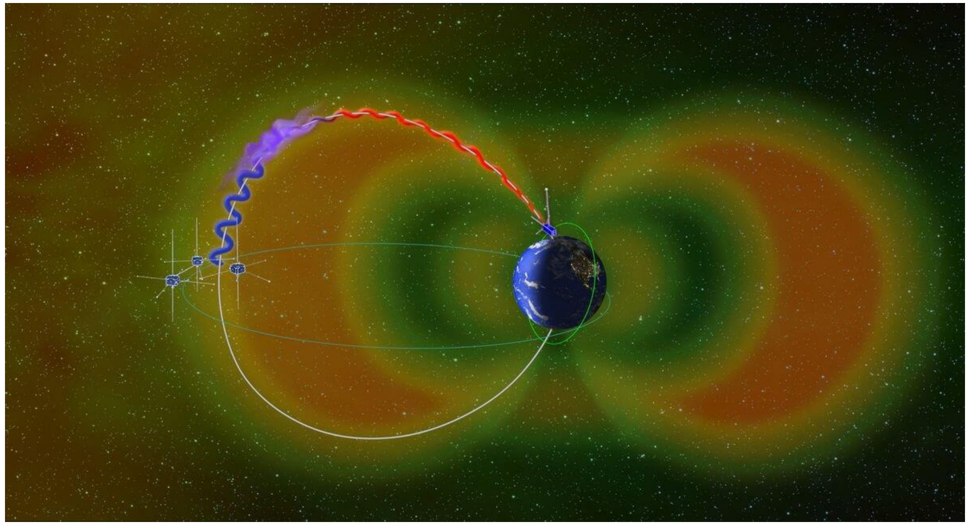

Original image Copyrights:
- *(Top) E.Mishin and A. Streltsov / Holzworth and Meng, NSSDC, NASA*
- *(Bottom) Zhang et al., Nature communications 2022*

Particle precipitation impacts in the ionosphere

- **Solar Energetic Protons (>10 MeV):**
  - Secondary particle showers in atmosphere (SEP>100 MeV)
  - D-layer absorption (SEP~10-100 MeV)
  - Stratospheric ozone destruction, climate impact
- **Electrons (3-20 keV):**
  - Auroras
  - Enhanced ionospheric conductances and currents
- **Electrons (30-1000 keV):**
  - D-layer absorption
  - Stratospheric ozone destruction, climate impact

Usually the electron content in the nightside D-layer is so low that radio waves do not notice it.

With energetic particle precipitation D-layer electron density enhances, but due to collisions with neutrals D-layer absorps the waves.

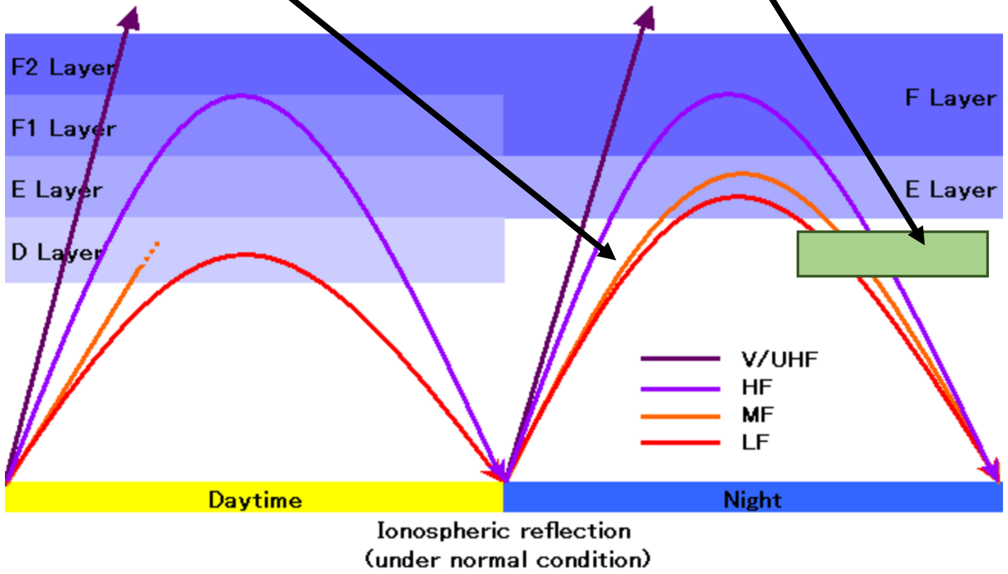

Original image Copyright: [By Muttley CC-BY-3.0 via Wikimedia Commons]

ILMATIETEEN LAITOS
METEOROLOGISKA INSTITUTET
FINNISH METEOROLOGICAL INSTITUTE

How attenuation by SEP is monitored: D-RAP tool

D-RAP tool:

- Inputs
  - solar X-rays (geostat orbit)
  - fluxes energetic protons (> 1 MeV) (geostat)
  - Kp index (geomagnetic activity, ground)
- Output:
  - Dayside D-layer absorption, "Short wave fadeout" (duration of some hours)
  - Polar Cap absorption (duration of days)
- Based on empirical formulas.
  - Reference: Sauer and Wilkinson, Space Weather, 2008, https://doi.org/10.1029/2008SW000399
  - Statistics for radiowaves at 30 MHz. Other frequencies achieved by scaling.

$$A_d = 0.155(J(E > Ec(InvLat))^{1/2},$$

$$A_n = 0.020(J(E > Ec(InvLat))^{1/2},$$

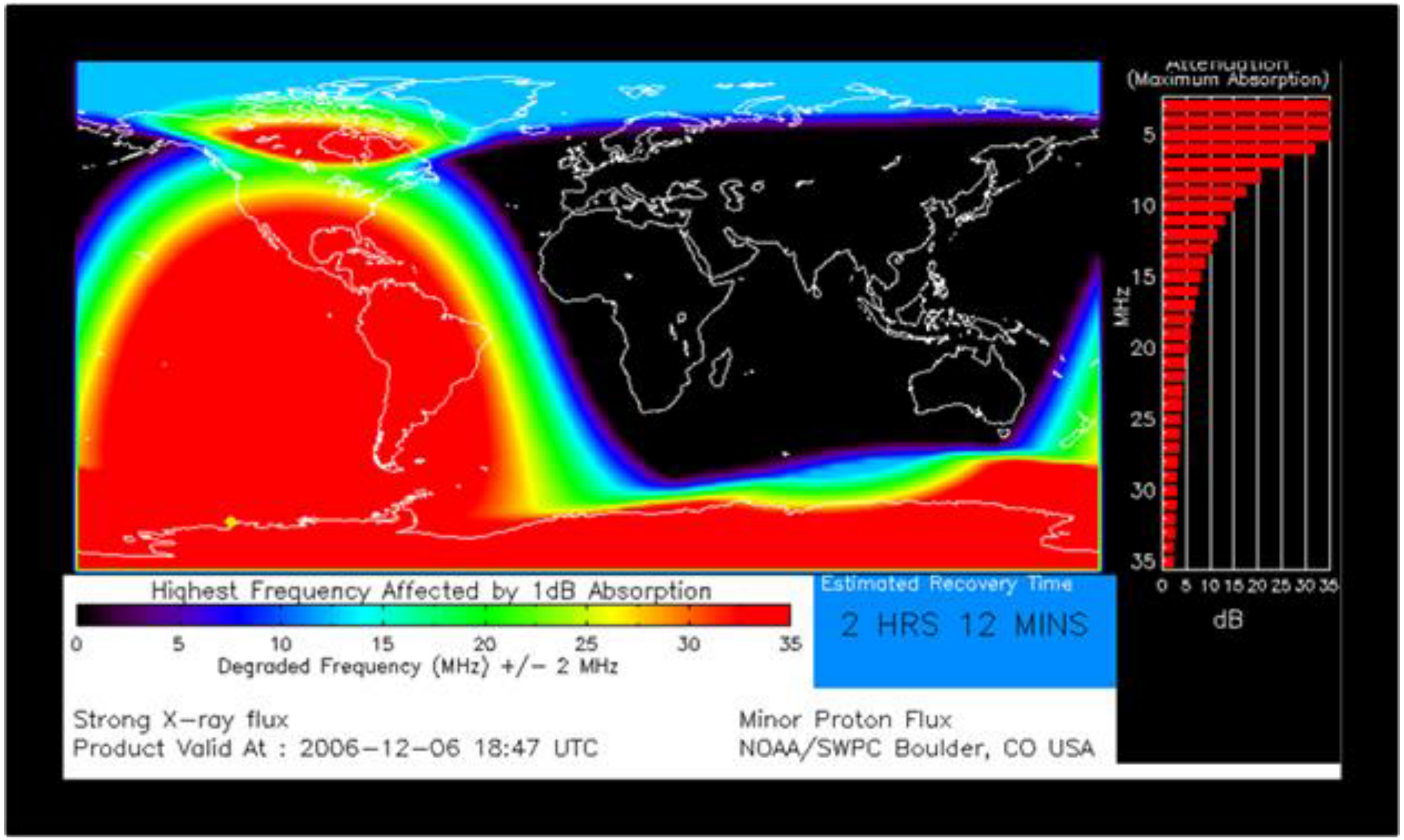

Figure: NOAA/UKMO

- *A_n and A_d absorption during night and day*
- *J(E>Ec) = energy flux of protons with energies above Ec*
- *InvLat= Latitude above which protons can reach ionosphere*

A similar approach under development for energetic electrons

Old satellite-riometer comparison studies from 1960s:

$A = 4\times10^{-3}\times(F(40))^{1/2}$ day time

(A in dB)

$A = 2\times10^{-3}\times(F(40))^{1/2}$ night time

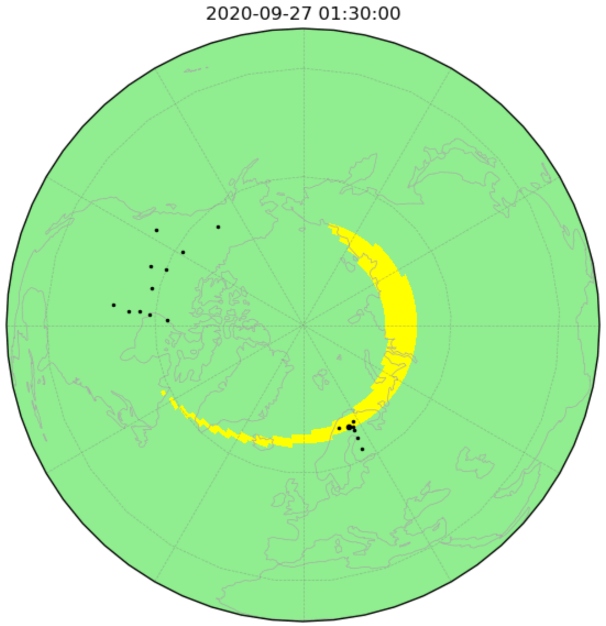

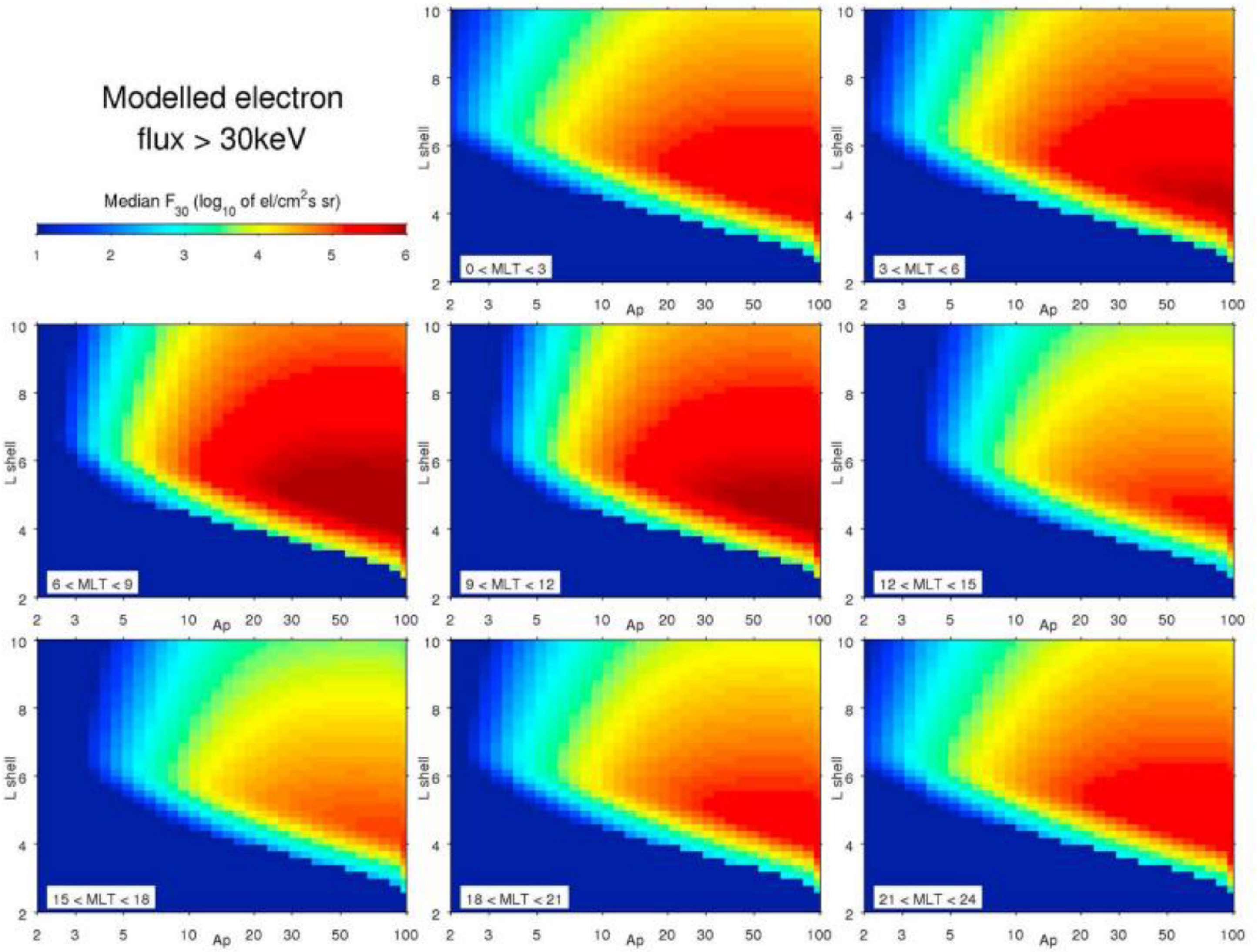

Figure 5. Median modeled flux >30 keV according to equation (8) (*MLT*-dependent model), as a function of *L* and *Ap* for eight *MLT* zones. *MLT* = magnetic local time.

Total electron flux for energies >E: $F(E)=F(F_{30}(MLT,L, Ap), k(MLT,L, Ap), E)$, where F30 = F(30)

Van de Kamp et al., 2014, https://doi.org/10.1029/2017JD028253

Riometer: A research instrument measuring cosmic noise absorption

- Passive receiver listening radiowaves (20-50 MHz) from stellar sources
- Background curve determined using quiet times
- Output: Deviations (in dB) from the background curves

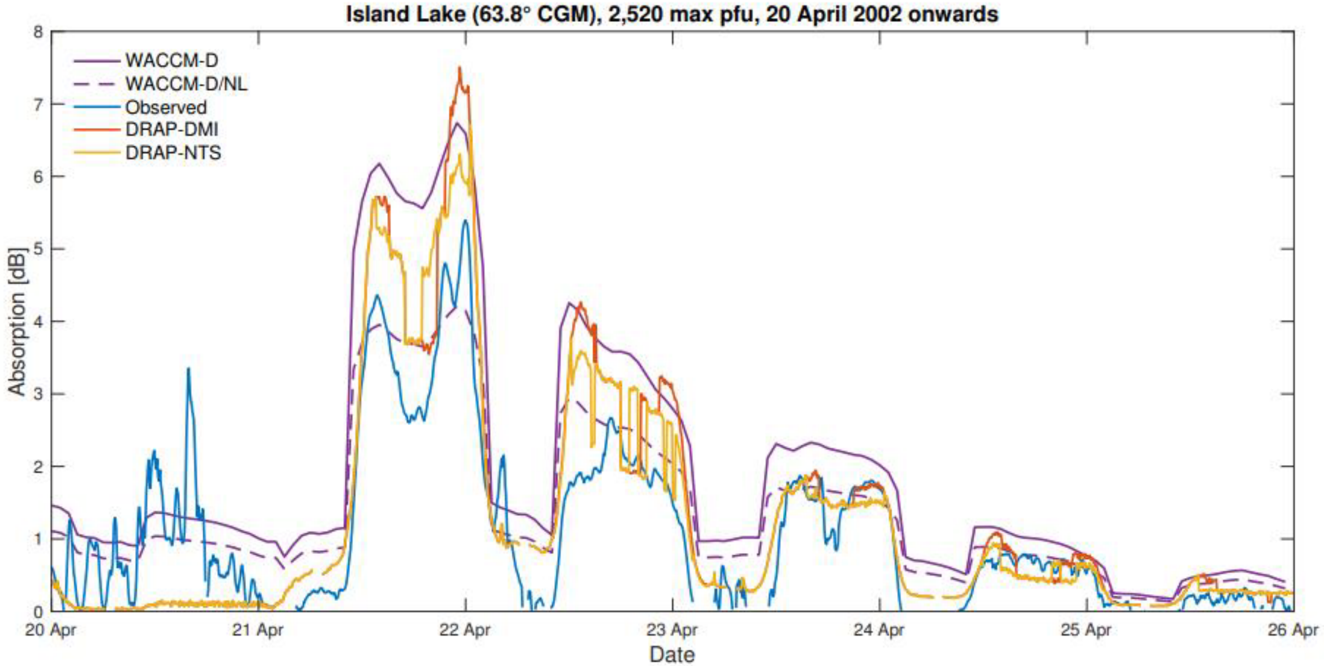

Figure 5.2: Modeled and observed cosmic noise absorption (CNA) at Island Lake during a solar proton event starting at 02:25 UT on 21 April 2002. Observed CNA is shown in blue, DRAP with the cutoff model by *Dmitriev et al.* (2010) is shown in orange, DRAP with the cutoff model by *Nesse Tyssøy and Stadsnes* (2015) is shown in yellow, CNA calculated from WACCM-D is shown in a purple solid line, and nonlinearity corrected from WACCM-D is shown with a purple dashed line.

Figures:
E. Heino, PhD thesis
RF Shamans Ltd
HAARP

The case of HF signal loss: Dilute ionosphere

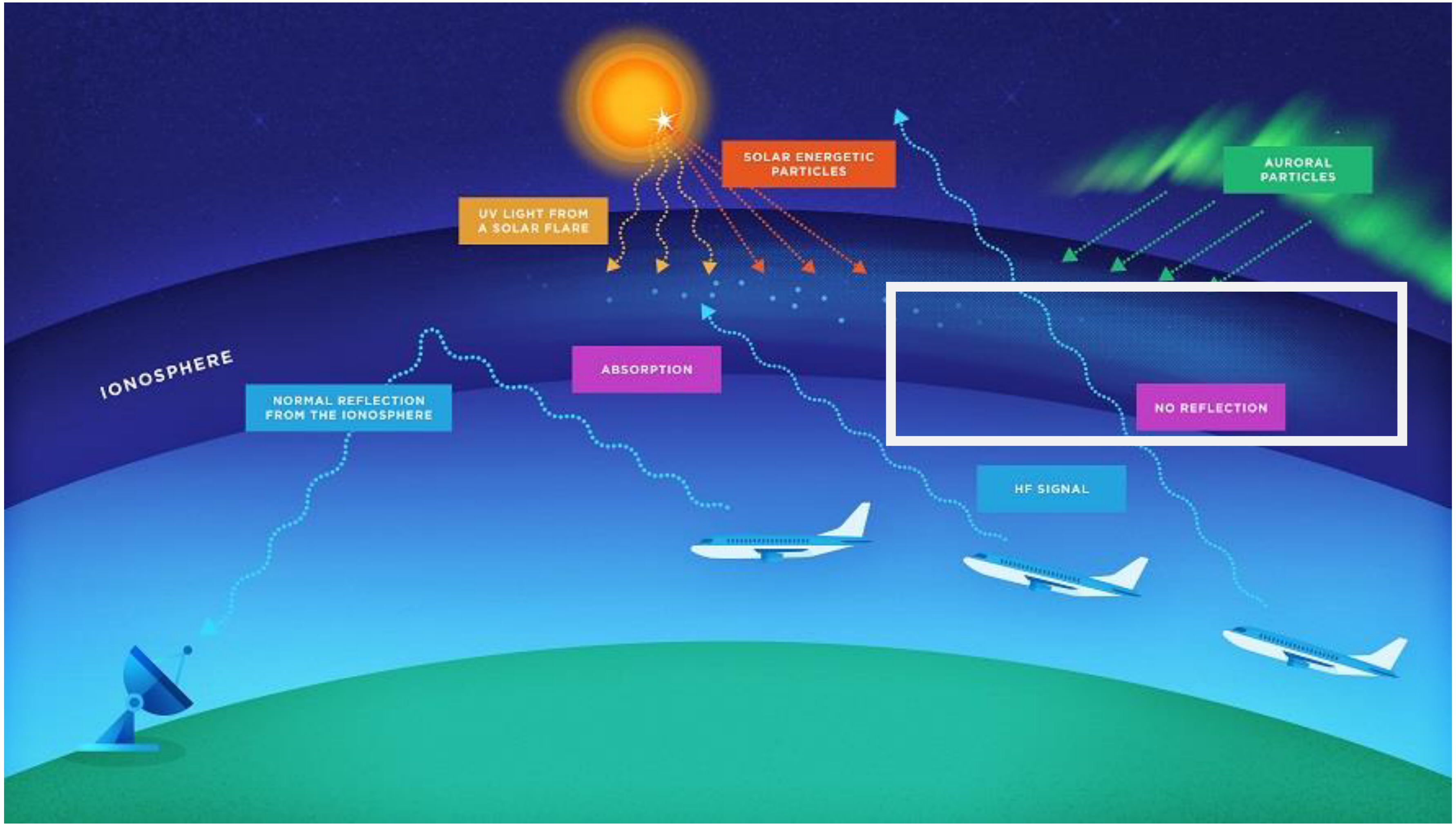

Drawing: FMI & STCE for PECASUS

Geomagnetic storm aftermath: plasma disappearing from the ionosphere

- Geomagnetic storm → Joule Heating in the high-lat ionosphere → thermospheric upwelling → change in the chemical composition at ionospheric F2 altitudes → enhanced recombination → electron density drops down

- Appearing during the main and recovery phases of a geomagnetic storm

- Pressure gradients → depression propagates from high to mid-latitudes. Propagation stronger during summer time.

- Causes drop in the Maximum Usable Frequency in HF communication.

- Impact stronger in the local time morning than afternoon. Duration 1-2 days

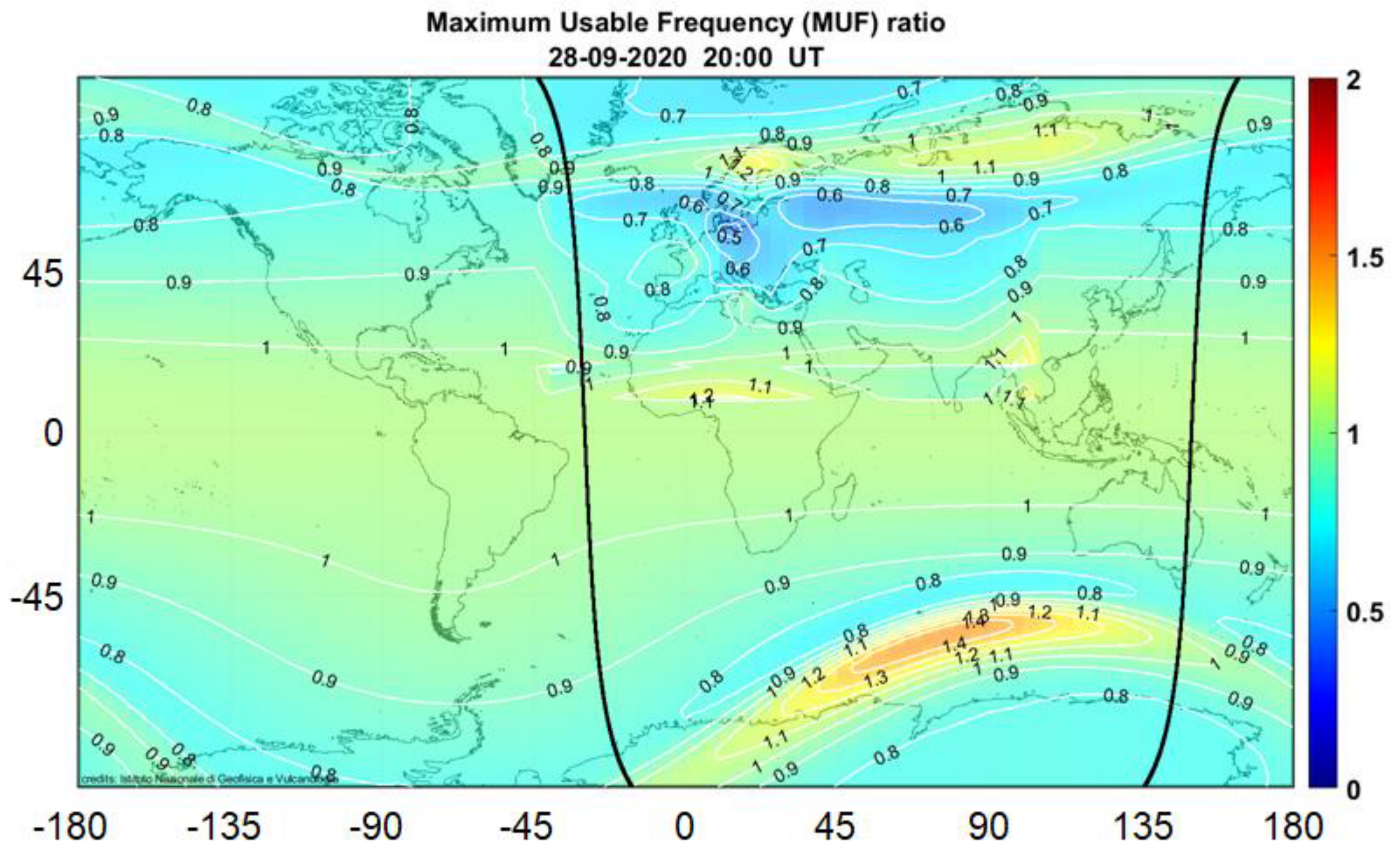

Figure: L. Perrone and D. Sabbagh, INGV

Ionosonde: A research instrument measuring altitude profile of ionospheric electron density

- A very traditional measurement concept since 1920's (Breit & Tuve 1925)
- Transmitter and receiver typically in same location -> vertical sounding
- Transmitting pulses with increasing frequencies in HF range (~0.5-25 MHz)
- Receiving signals with varying delays → estimate of the reflection altitude (propagation speed of light assumed)
- Assumption: the wave reflects back at the altitude where is frequency is equal to the critical plasma frequency

$$\omega_N = [Ne^2/\varepsilon_0 m_e]^{1/2}.$$

Slide: based on slide by Johannes Norberg (FMI)

Photo: Dynasonde in Tromsö (Chris Hal

Ionosonde

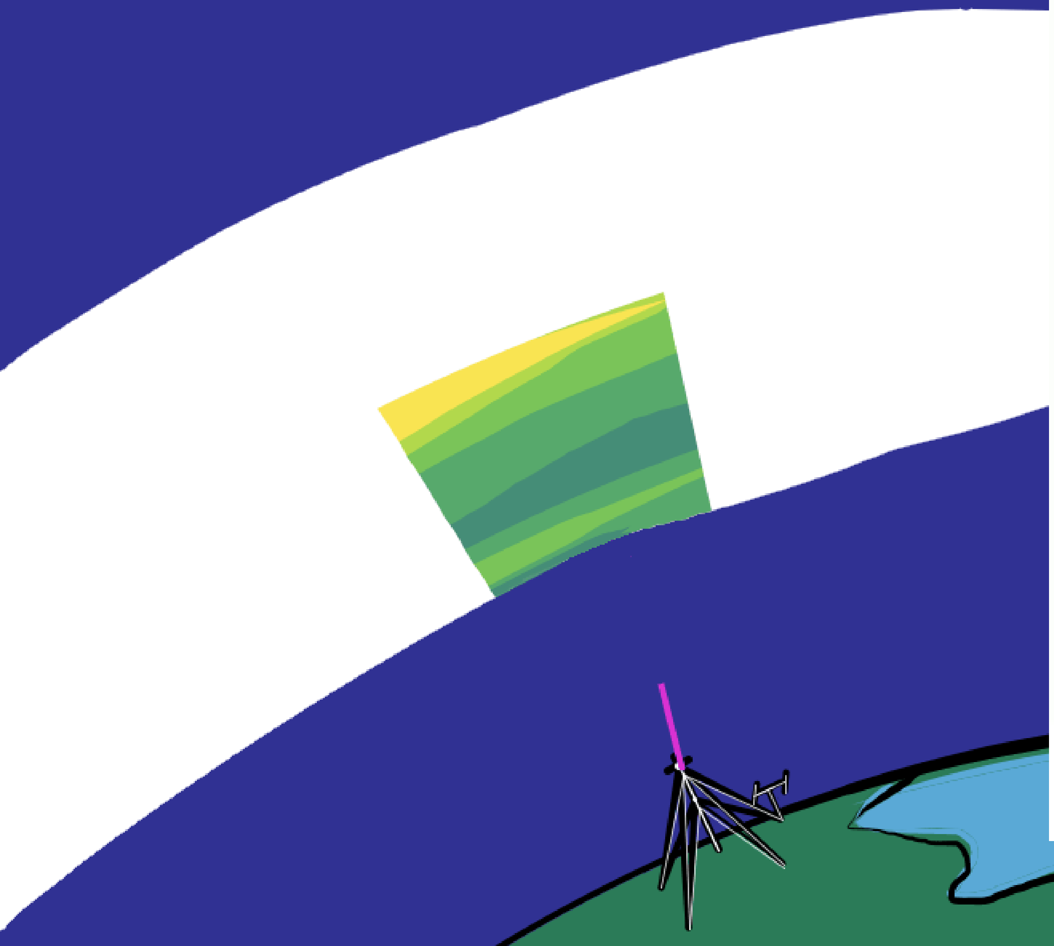

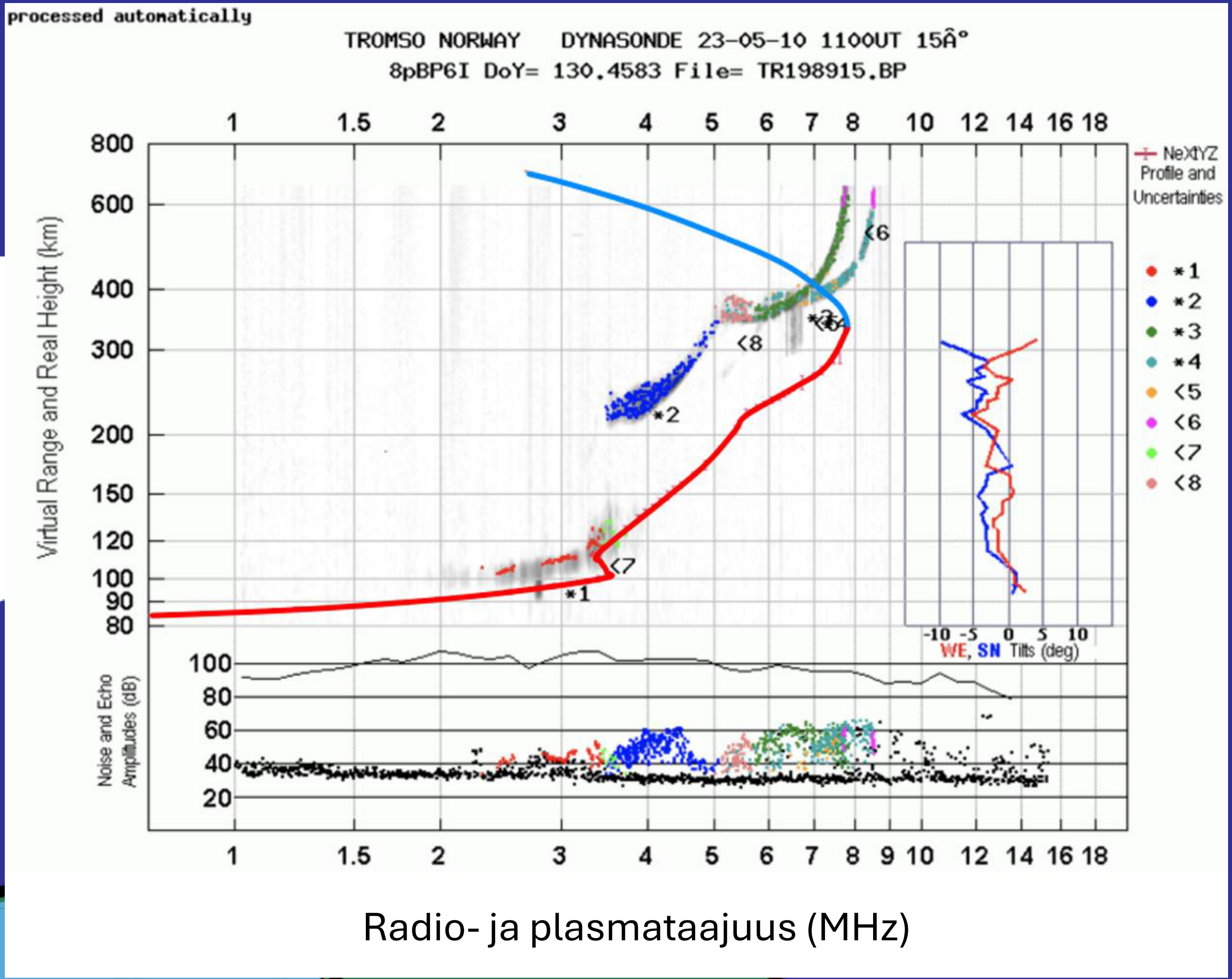

Slide: Johannes Norberg (FMI)

Examples of space weather effects

Impacts on radio waves in GHz range

Brief Intro: Global Navigation Satellite Systems (GNSS)

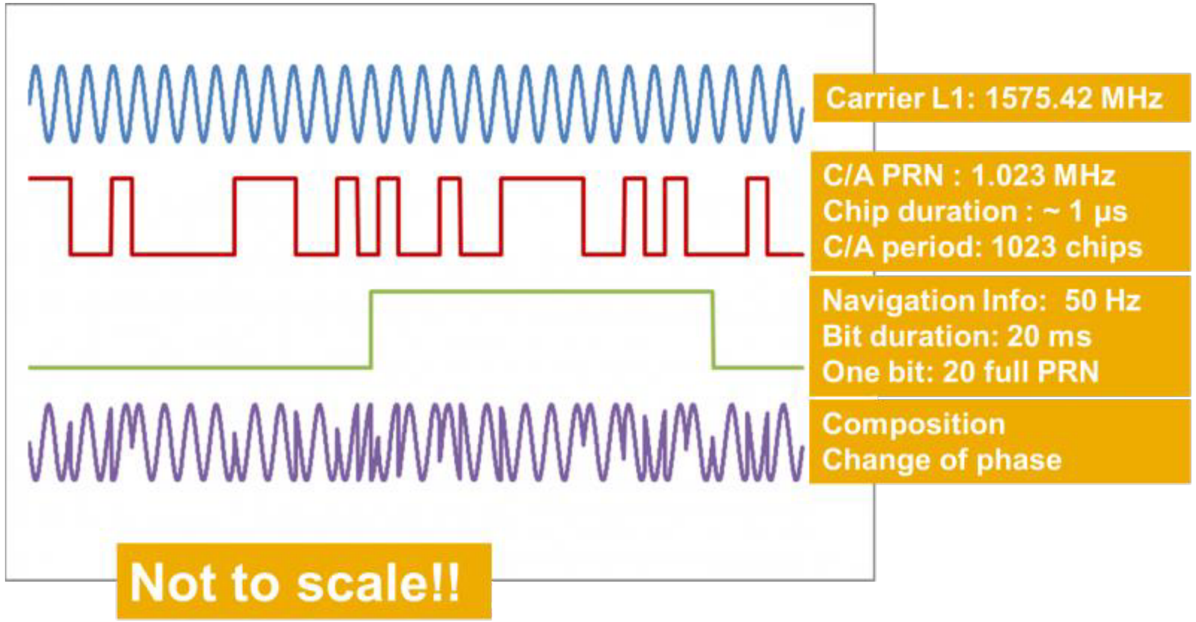

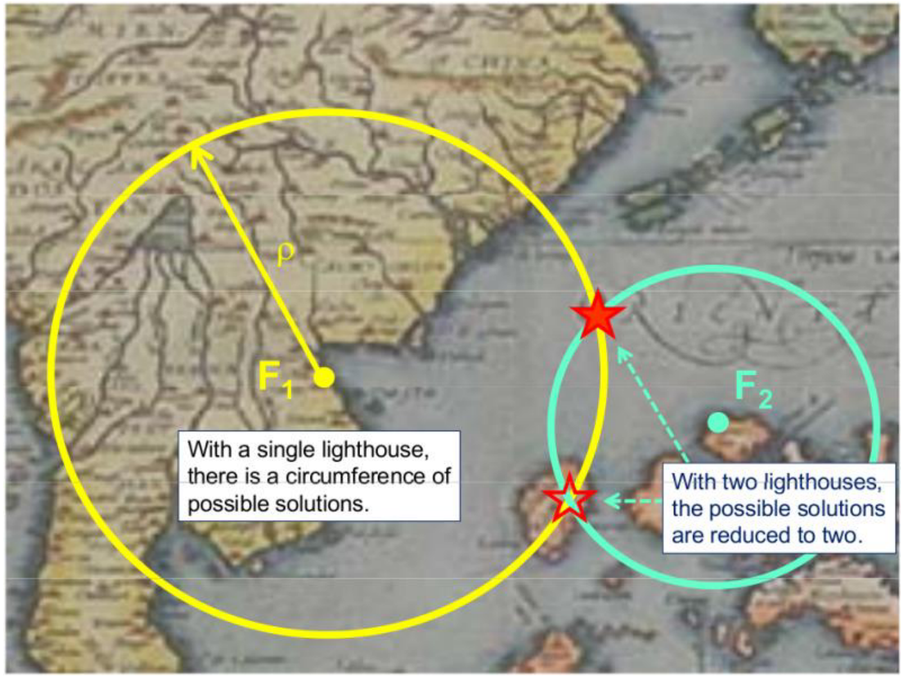

GPS Signal composed of:

- Carrier waves with two frequencies:
  - L1 1575.42 MHz & L2 1227.60 MHz
- Pseudo-Random noise: information about signal travel time
- Navigation data: satellite location, clock bias, etc.

Analogy in 2D: A ship listening acoustic signals from two lighthouses. If signal is received with 20 s delay the pseudorange estimate (ρ) is 340 m/s*20 s=6.8 km

Source: ESA navipedia

GNSS basic observables & combinations

Basic observables:

- **Pseudorange:** Estimate of distance by Rp=c(t_r-t_s), t_r= the time of signal reception & t_s=the time of signal transmission

$$R_p = \rho + c(dt_r - dt^s) + T \boxed{+ \alpha_f\, STEC} + K_{P,r} - K_P{}^s + \mathcal{M}_P + \varepsilon_p$$

- **Carrier phase:** Estimate of distance by the phase of carrier. Included ambiguity by N*λ, where λ is the carrier wavelength and N is an unknown integer.

$$\Phi_L = \rho + c(dt_r - dt^s) + T \boxed{- \alpha_f\, STEC +} k_{L,r} - k_L{}^s + \lambda_L N_L + \lambda_L w + m_L + \epsilon_L$$

$$\alpha_f = \frac{40.3}{f^2} 10^{16}\ m/TECU$$

STEC = Total electron content along signal path [TECU]; TECU = $10^{16}/m^3$

- **Doppler shift:** Doppler shift in carrier. Estimated by the relative velocity between receiver and transmitter

Ionosphere-free combination:

$$\Phi_{LC} = \frac{f_1^2\, \Phi_{L1} - f_2^2\, \Phi_{L2}}{f_1^2 - f_2^2} \quad ; \quad R_{PC} = \frac{f_1^2\, R_{P1} - f_2^2\, R_{P2}}{f_1^2 - f_2^2}$$

Geometry-free combination: $\Phi_{LI} = \Phi_{L1} - \Phi_{L2} \quad ; \quad R_{PI} = R_{P2} - R_{P1}$

Source: ESA navipedia

GNSS measurements

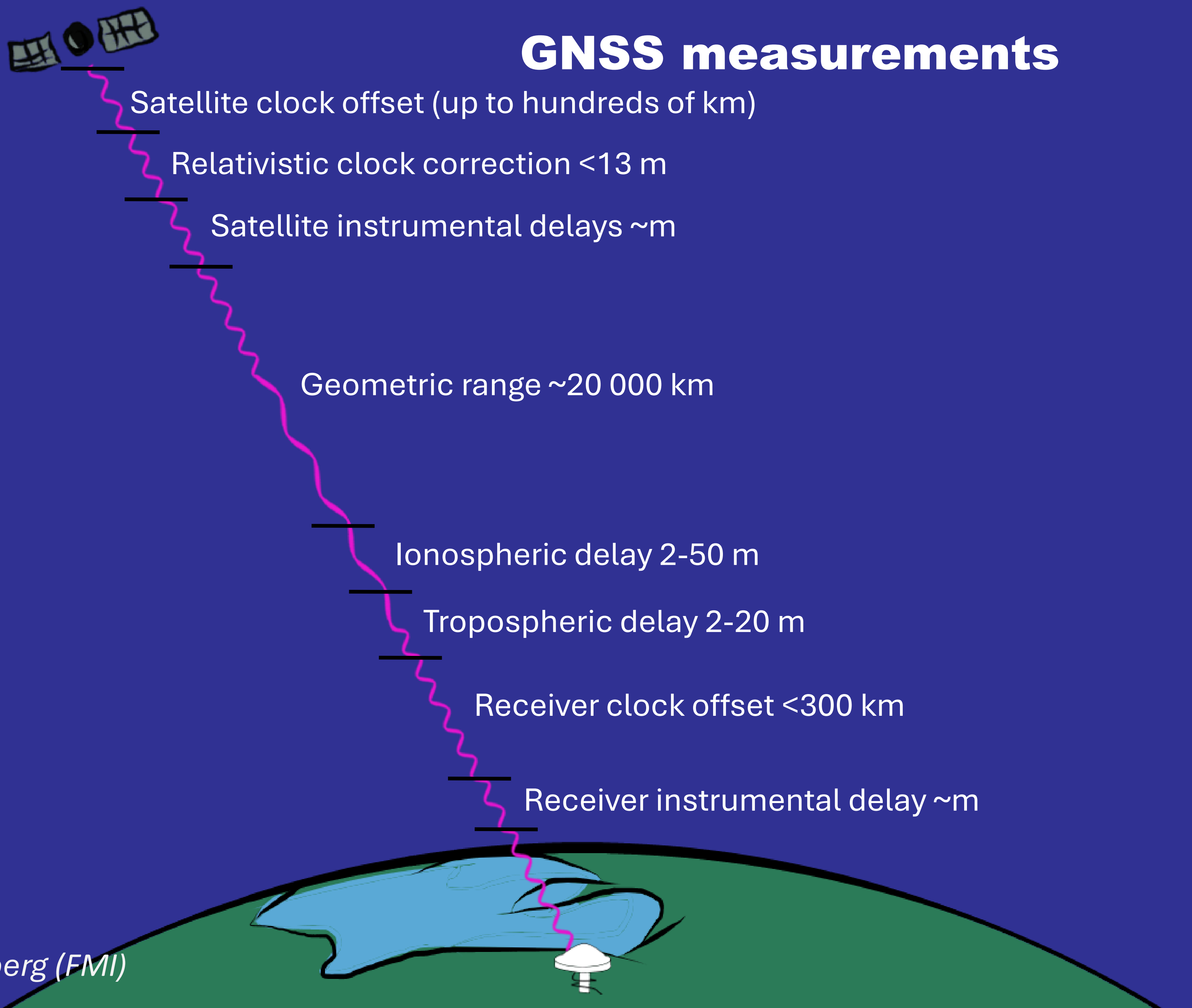

(Navipedia)

Slide: Johannes Norberg (FMI)

GNSS measurements

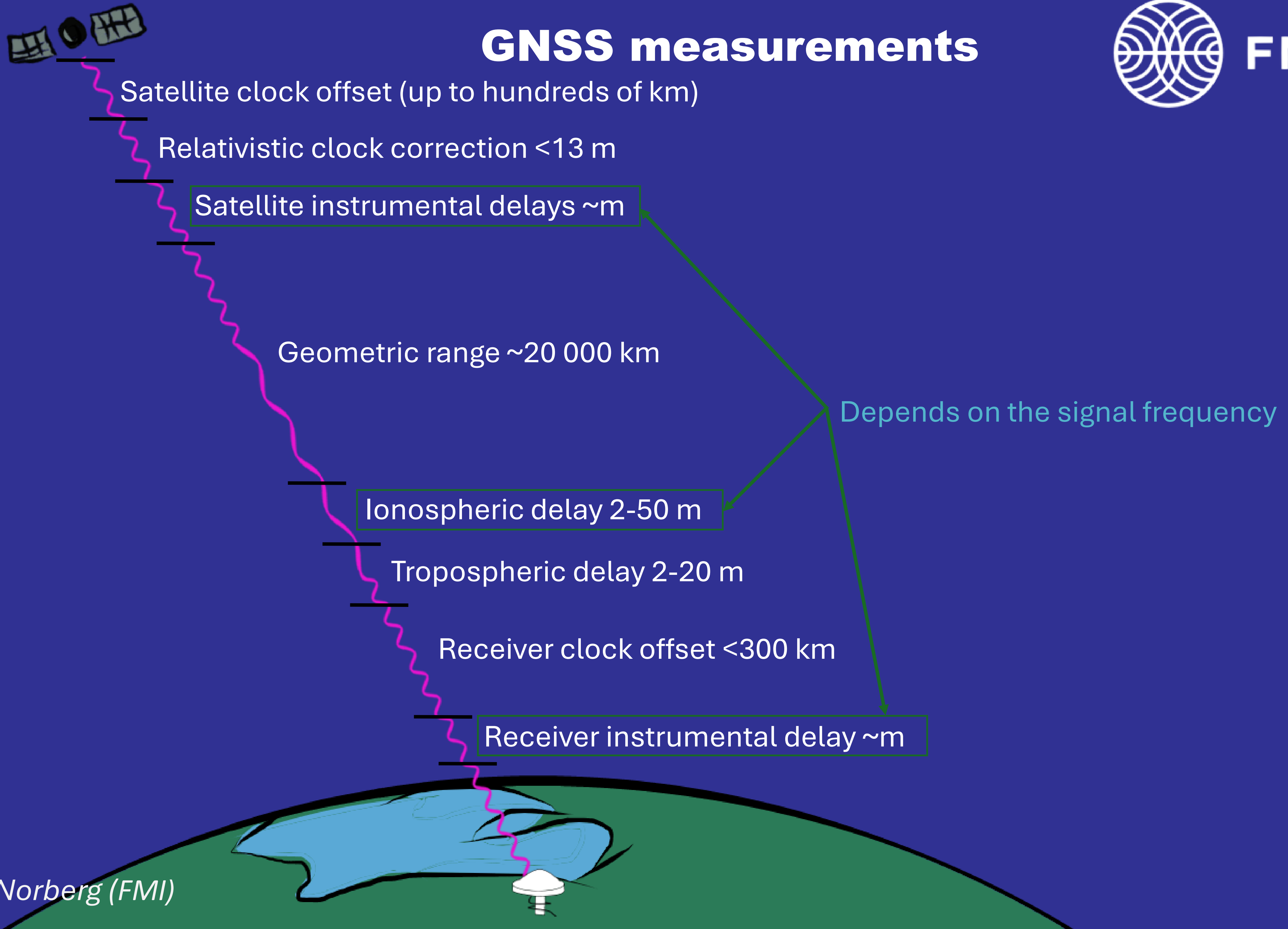

Slide: Johannes Norberg (FMI)

EGNOS improves GPS over Europe

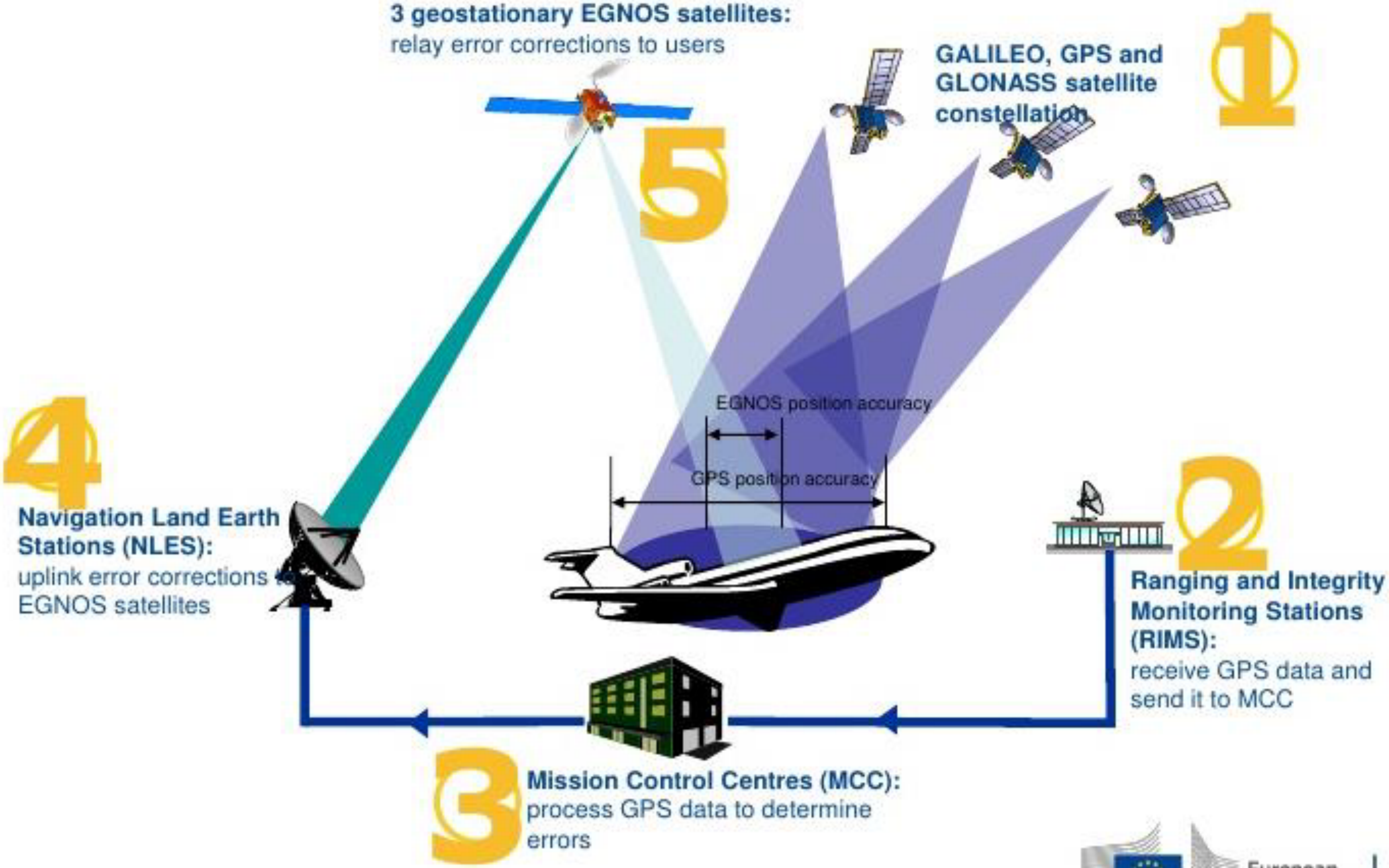

European Commission

The case of GNSS signal diffraction: Ionospheric scintillation

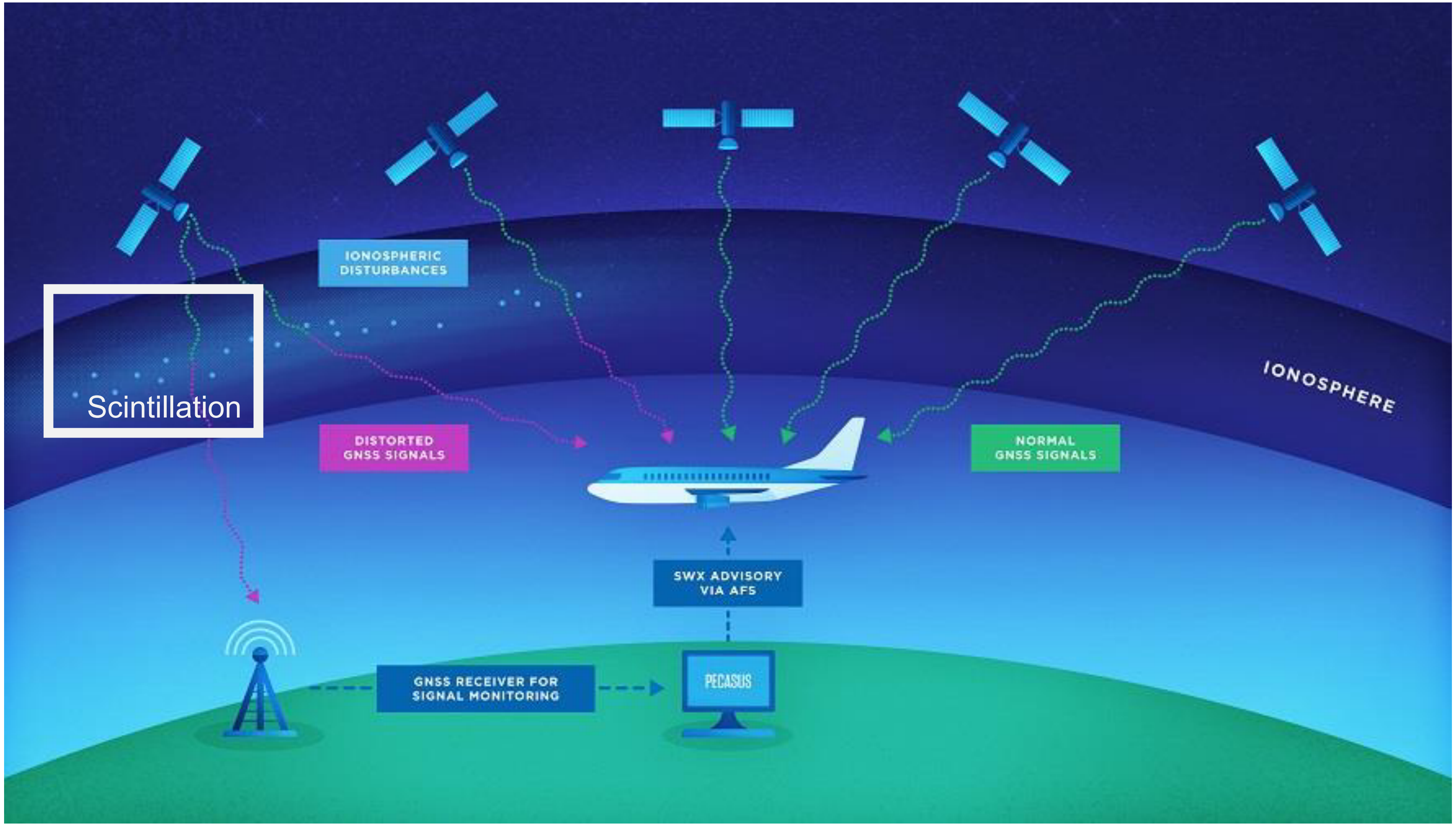

Drawing: FMI & STCE for PECASUS

Small structures (some hundreds of m) in the ionospheric electron density cause relative phase shifts in the GNSS signal wave front

Animation: Bath University

A solar burst of X-rays and EUV on Sep 9 2017 caused
Disturbances in the ionosphere →
Performance of Galileo augmentin system dropped
down for one hour.

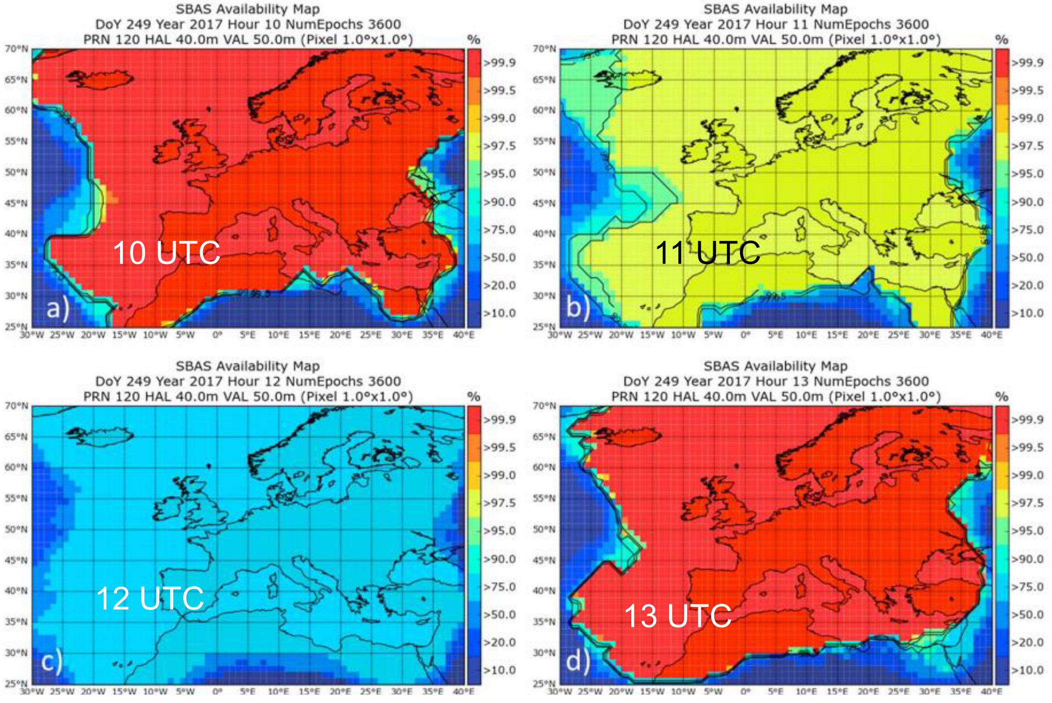

Figure: Berdermann et al. (2018), ESA

Red= Nominal support for Galileo
Other colors= Decreased support for Galileo

GNSS receivers monitoring small scale ionospheric structures

- Monitoring of small scale ionospheric structures and consequent scintillation can be done with specific scintillation receivers with high sampling rates (50 Hz).
- High resolution (50 Hz) receivers are used to derive parameters that characterize the the strength of scintillation in amplitude (S4) and in phase (σ_ϕ).
- Standard resolution receivers (1 Hz) are used to derive Rate of TEC and Rate of TEC index (ROTI) which also characterize rapid variations in the ionosphere

S4 (dimensionless): Standard deviation of L1 carrier S/N computed typically determined with 1 min resolution

σ_φ(rad): Standard deviation of de-trended L1 carrier phase typically determined with 1 min resolution

ROTI (TECU/min): Standard deviation of rate of TEC typically determined with 1 or 5 min resolution

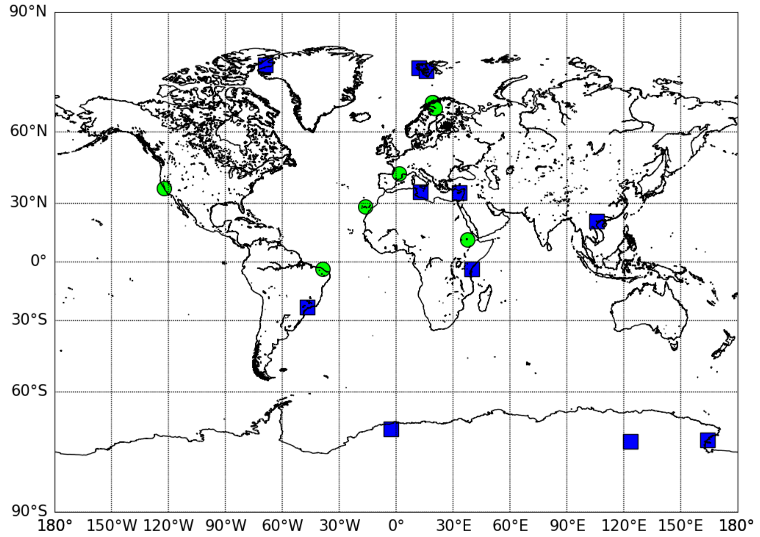

Figure (up): The scintillation receiver stations used in the PECASUS service (Kauristie et al., 2021)

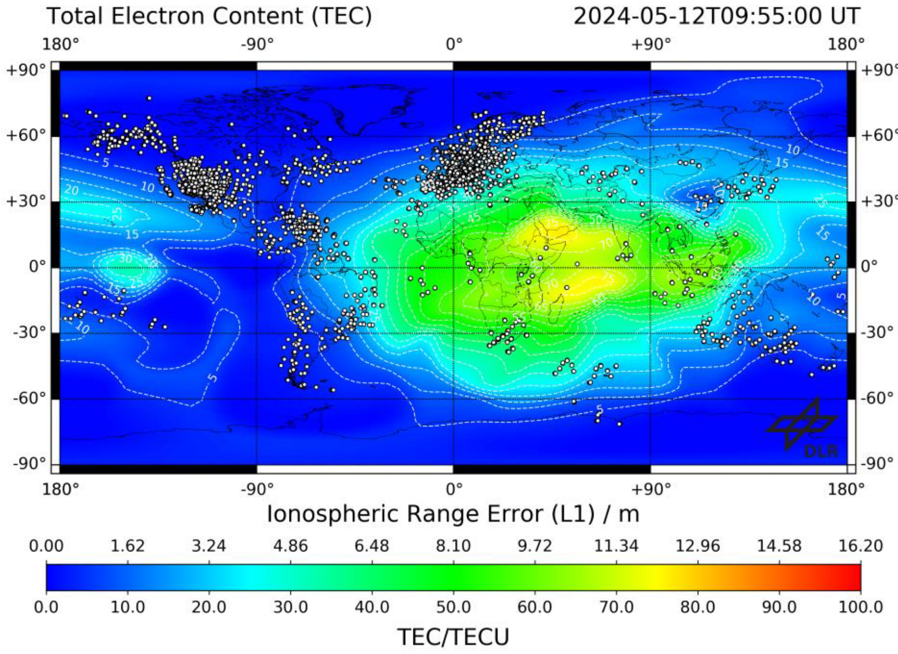

Figure (right): A TEC map by the IMPC service maintained by DLR showing also the network of GNSS standard receivers that can be used to derive ROTI

An example: Space weather storm on Feb 26-27, 2023

- Two solar flares on Feb 24 and Feb 25→ Impact by two combined Coronal Mass ejections → Geomagnetic storm during Feb 26-Feb 28→ Disturbed ionosphere

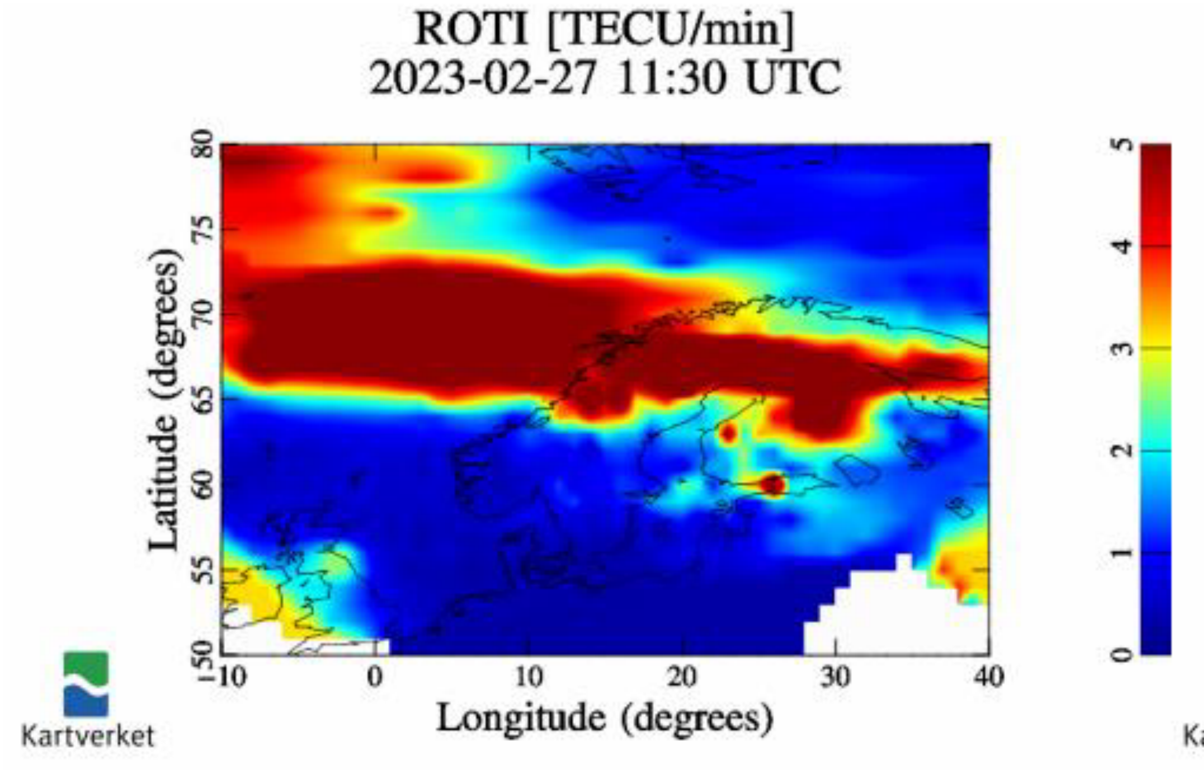

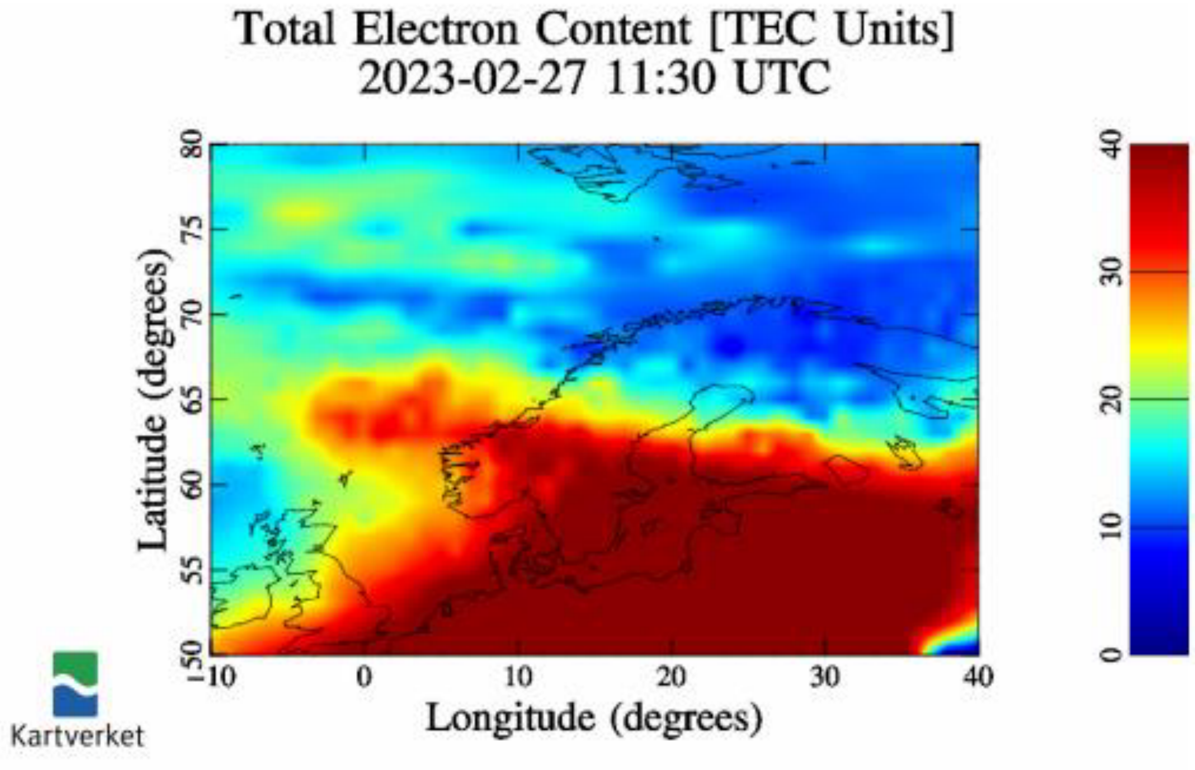

Plots: Norwegian Mapping Authority

Impact in accurate positioning around noon on Feb 27: Finland

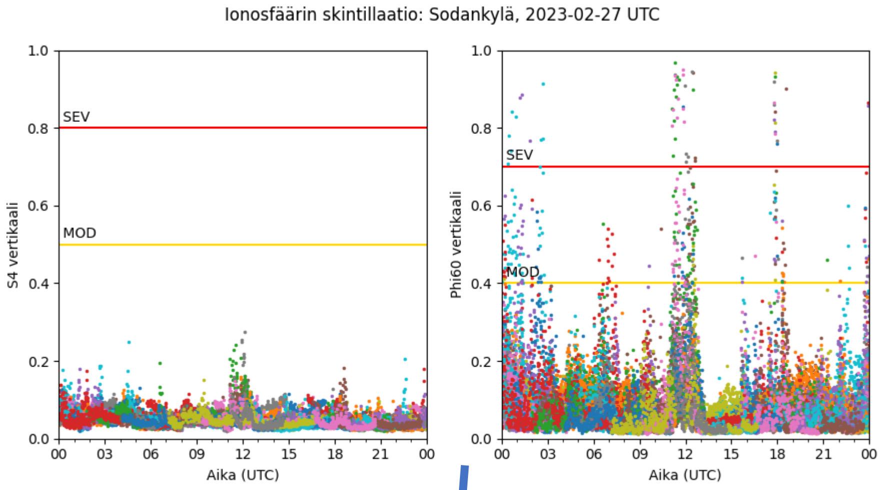

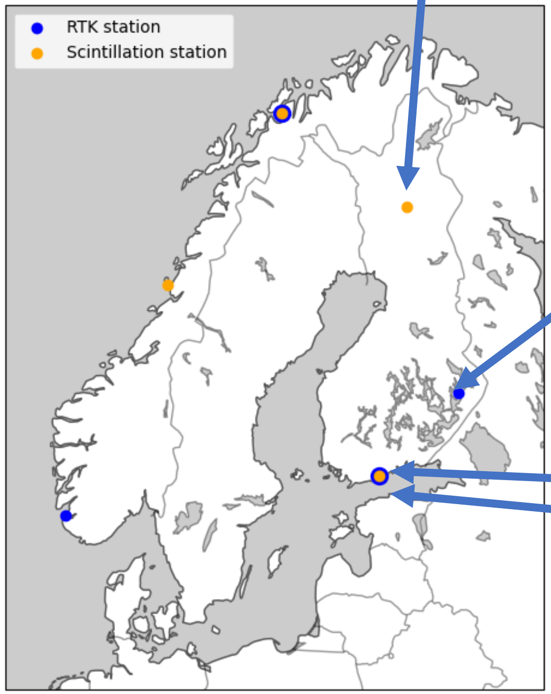

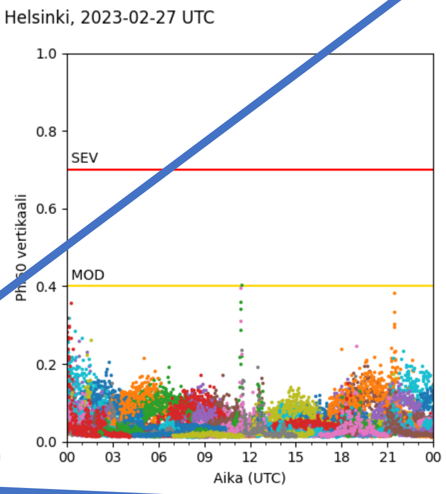

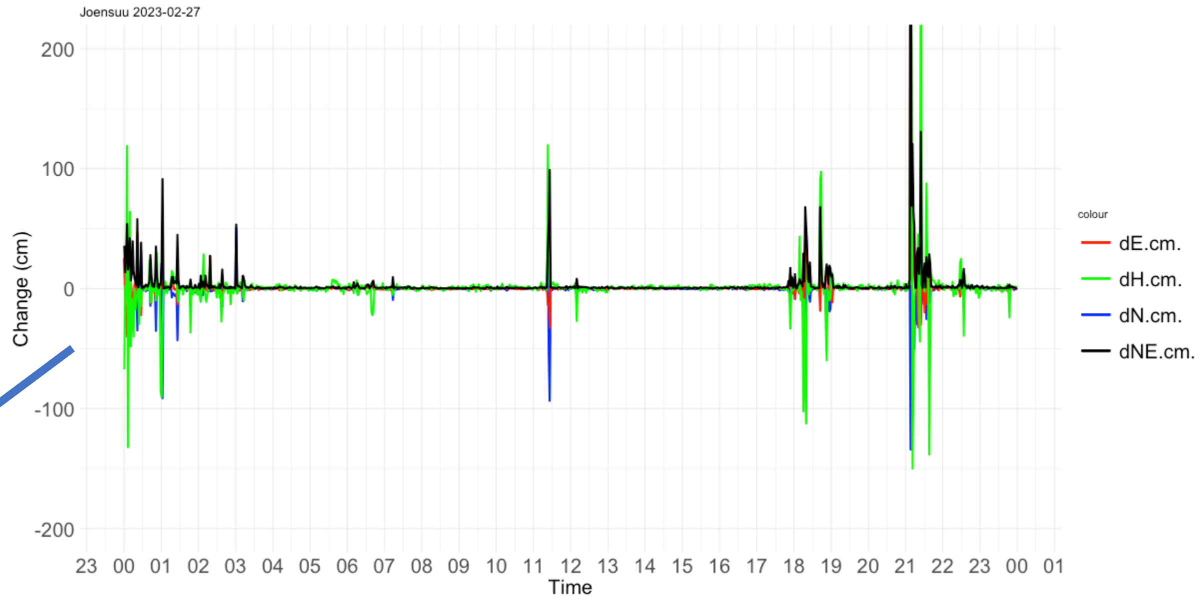

Plots: FINPOS and FMI

The case of GNSS dispersion : Ionospheric delay

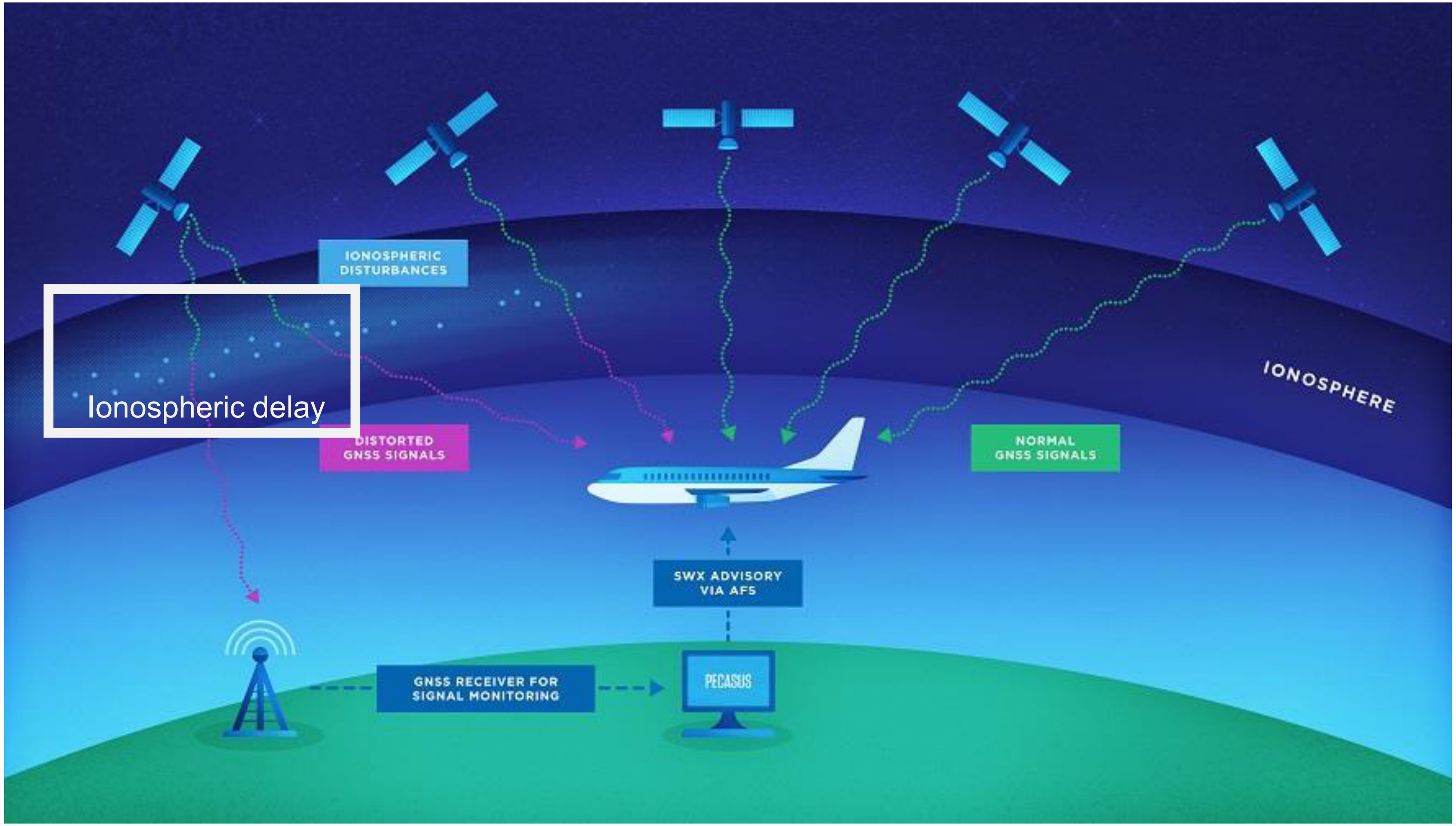

Drawing: FMI & STCE for PECASUS

GNSS as a system supporting Space Weather monitoring

- The geometry free phase combination of L1 and L2 signals can be used to derive Total Electron Content along the signal path from the satellite to the ground-based receiver.
- Slant TEC (STEC) is TEC along the path
- Vertical TEC (VTEC) is STEC converted to TEC along a vertical path with a geometric conversion factor
- Ionospheric Piercing Point (IPP) is the point where the signal crosses the ionosphere at ~350 km altitude

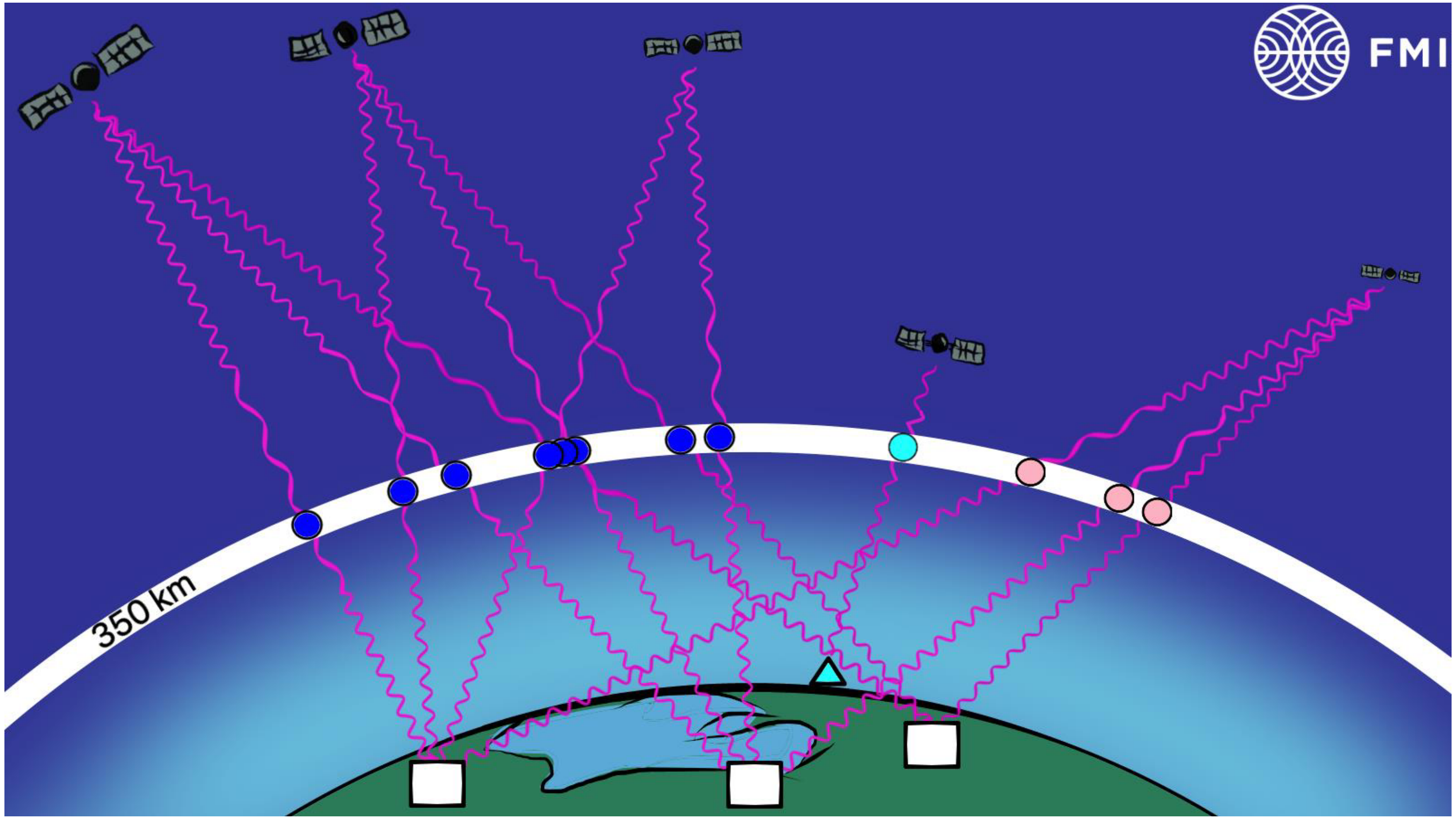

Figure: Johannes Norberg, FMI

Ionospheric Tomography based on radio waves reflecting and passing through the ionosphere

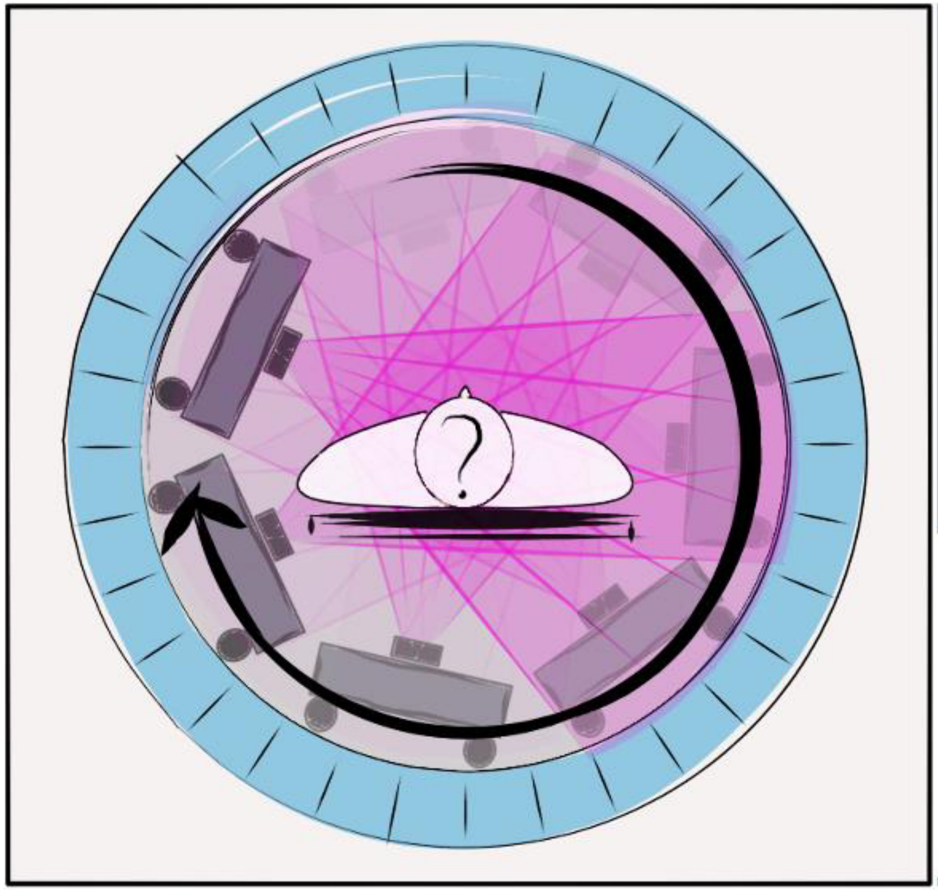

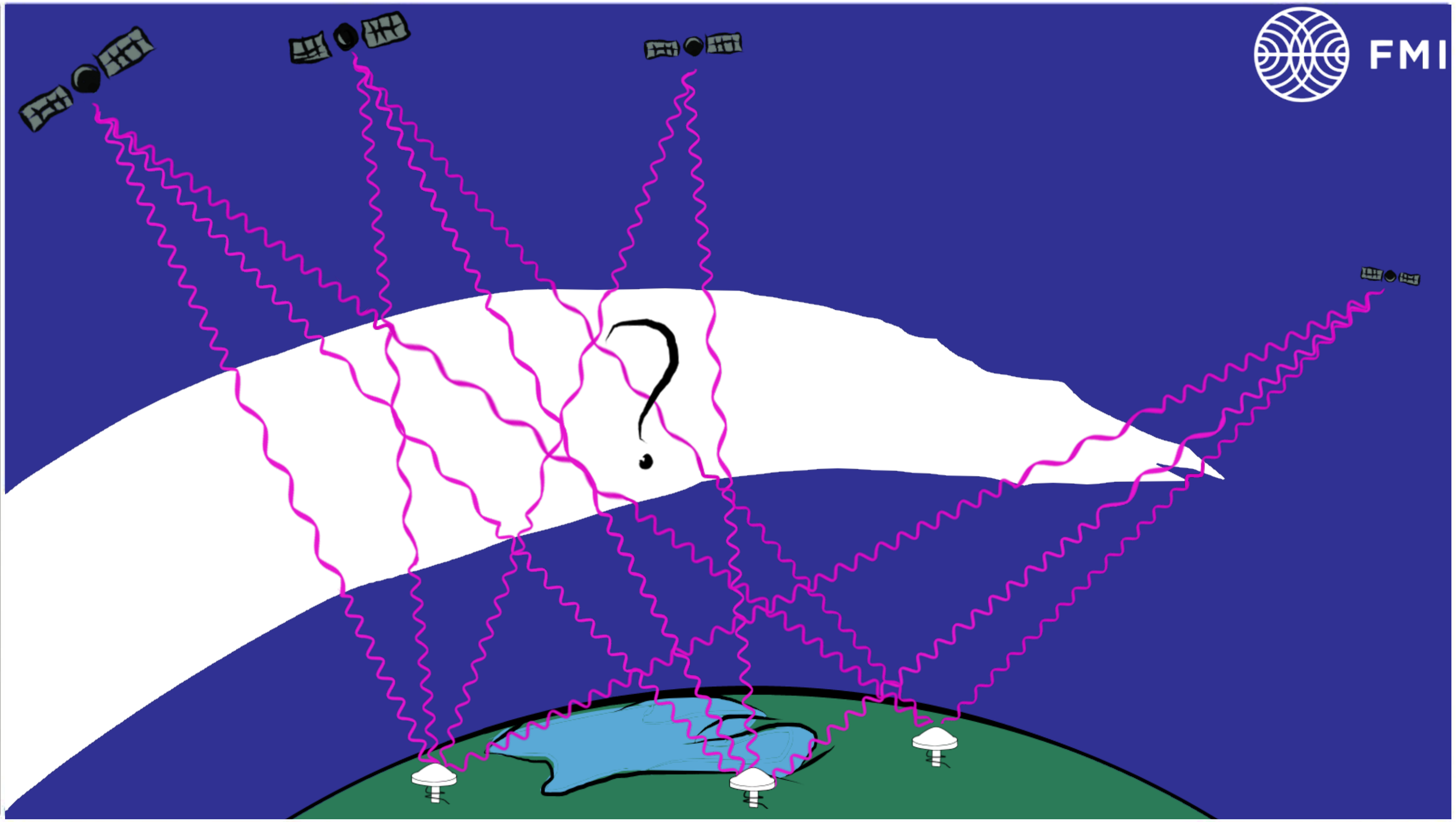

Slide: Johannes Norberg (FMI)

Statistical inversion -> 3D ionospheric imaging

Little information on the vertical structure → Additional regularizing information is needed → ionosondes' support used

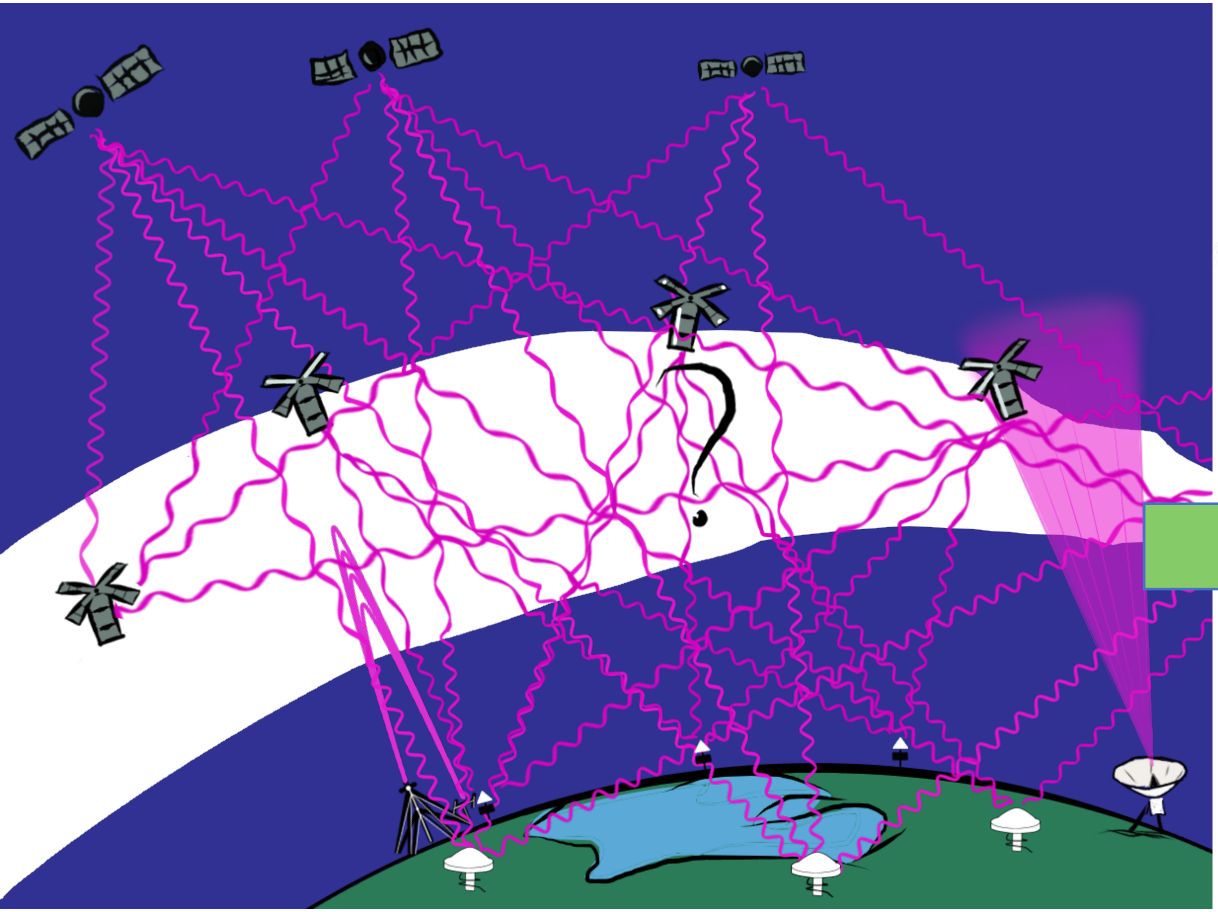

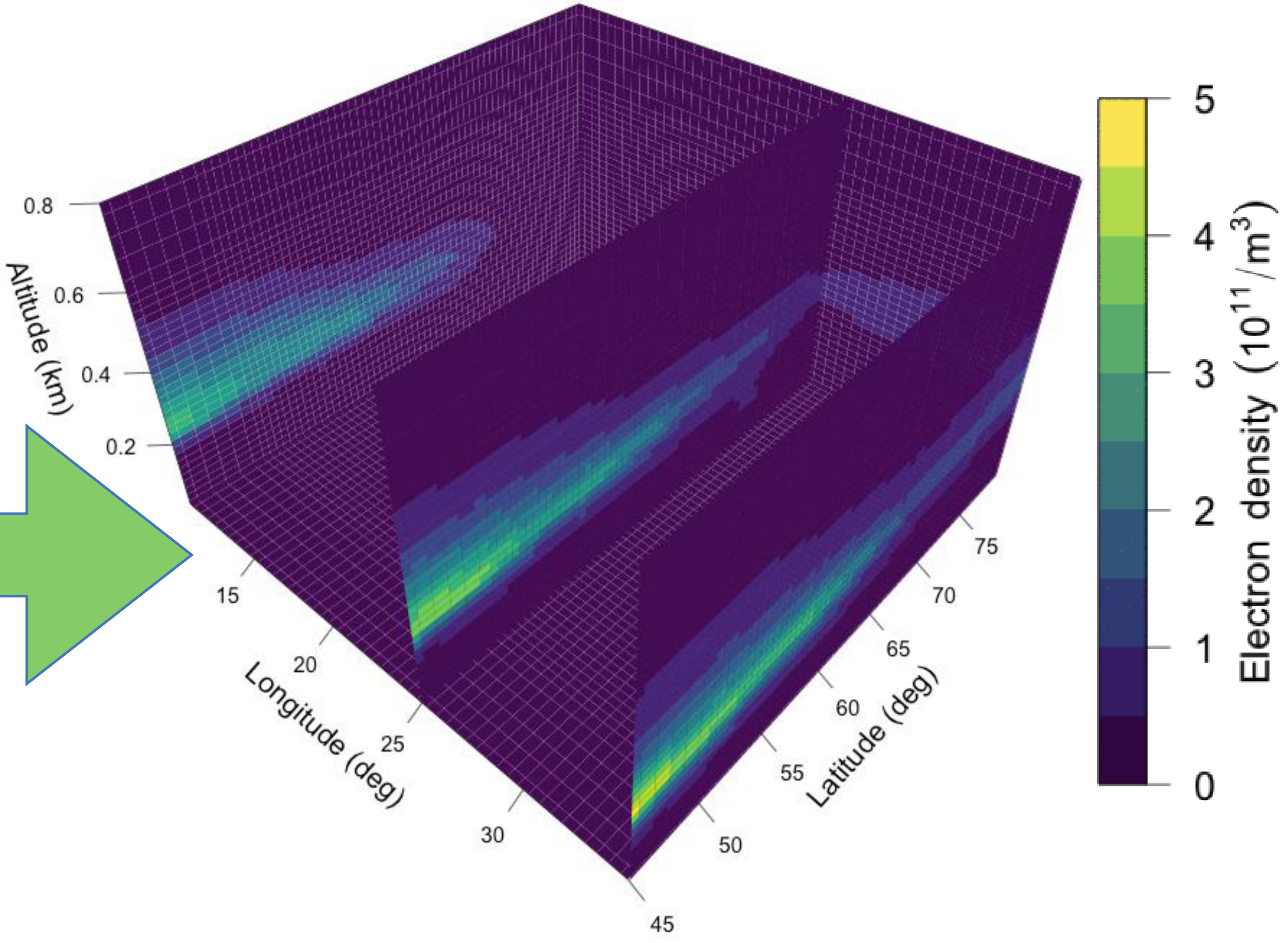

Slide: Johannes Norberg (FMI)

Examples of services impacted by problems in accurate positioning

- In Norway, sheep are let out freely to graze in open fields every summer.
- Since the sheep tend to wander in small herds over large geographical distances, it can be a demanding task for the farmer to keep track of his own animals.
- Findmy produces electronic bells with satellite tracking for livestock on pasture. With this electronic bell the owner of the livestock has a full overview of where the livestock are at all times.
- Opportunity for space weather services: Collecting sheep back to shelters before cold winter should be arranged during calm space weather conditions

find◦my

- Autonomous runway sweepers operated at the Oslo Airport Gardemoen
- Tests conducted in winter 2022/2023
- Test campaign during the night March 23-24, 2023 had to be interrupted due to problems in RTK positioning
- Checking NMA ROTI service revealed that ionospheric disturbances were the cause for the problems in RTK positioning
- Lesson learned: Forecasts of space weather situation will be used when selecting runway and taxiway sweeping approaches (automated/manual) in full scale operations

Ionospheric storm products in space weather services

Examples collected on May 12, 2024 after a sequence of several X-class solar flares

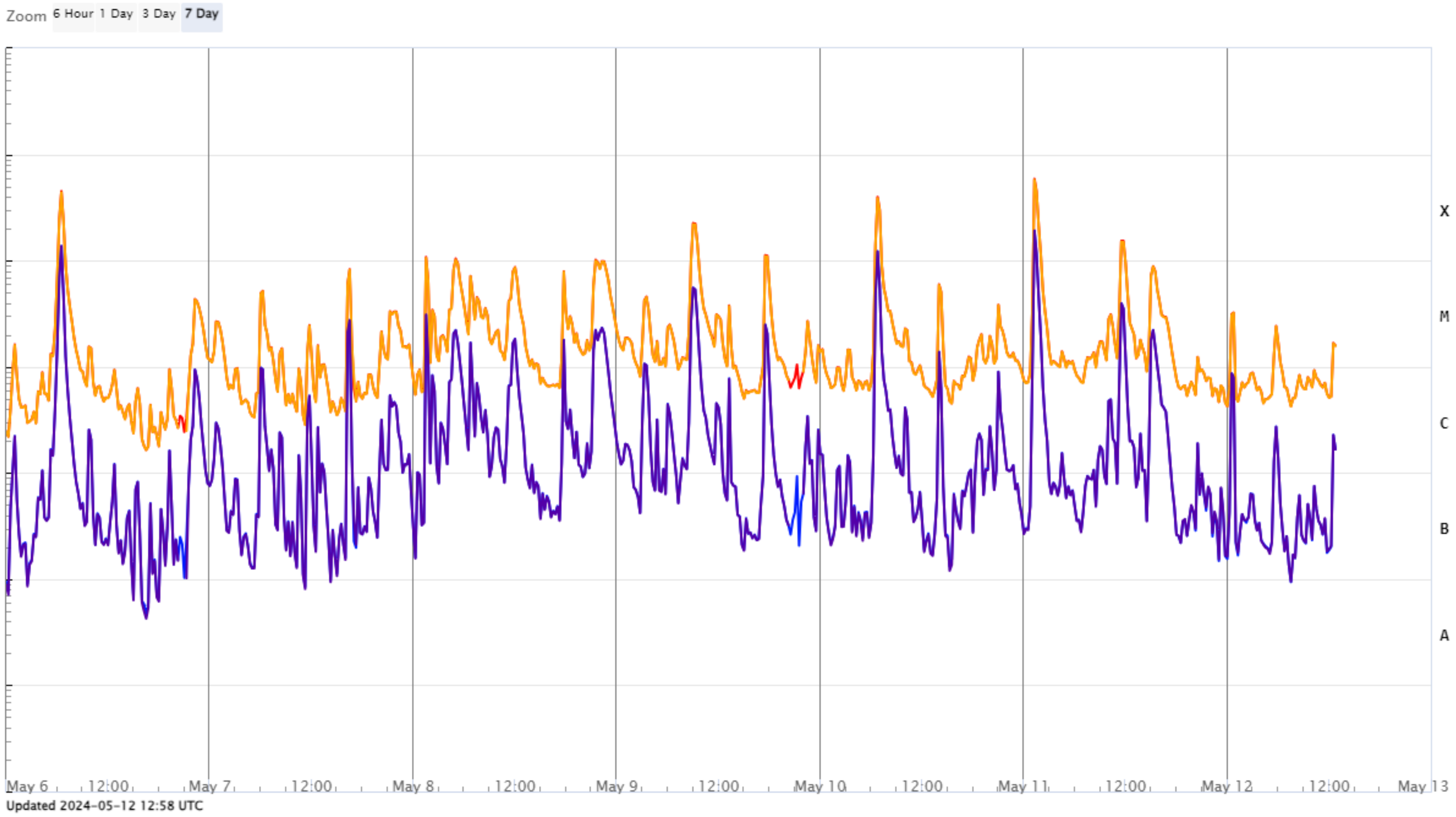

Space Weather Prediction Center (SWPC), USA:

Currently quiet, but enhanced probabilities for problems in HF communication foreseen both in dayside and high-lat ionospheres

SPACE WEATHER PREDICTION CENTER
NATIONAL OCEANIC AND ATMOSPHERIC ADMINISTRATION

Sunday, May 12, 2024 13:06:05 UTC

HOME | ABOUT SPACE WEATHER | PRODUCTS AND DATA | DASHBOARDS | MEDIA AND RESOURCES | SUBSCRIBE | ANNUAL MEETING | FEEDBACK

Search

Nowcast

SPACE WEATHER CONDITIONS on NOAA Scales

24-Hour Observed Maximums

R2	S2	G4
moderate	moderate	severe

Latest Observed

R	S	G
none	none	none

Predicted 2024-05-12 UTC

R1-R2	95%	S1 or greater	60%	G4
R3-R5	75%			severe

G=Geomagnetic storm impacts

S=Solar radiation storm impacts

R=Radio black-out impacts

Forecast for the coming days

SPACE WEATHER CONDITIONS on NOAA Scales

Predicted 2024-05-12 UTC

R1-R2	95%	S1 or greater	60%	G4
R3-R5	75%			severe

Predicted 2024-05-13 UTC

R1-R2	95%	S1 or greater	60%	G3
R3-R5	75%			strong

Predicted 2024-05-14 UTC

R1-R2	15%	S1 or greater	5%	G1
R3-R5	5%			minor

National Institute of Communication and Information Technology (NICT), Japan:

Decreases in ionospheric electron density starting on the evening of May 10.

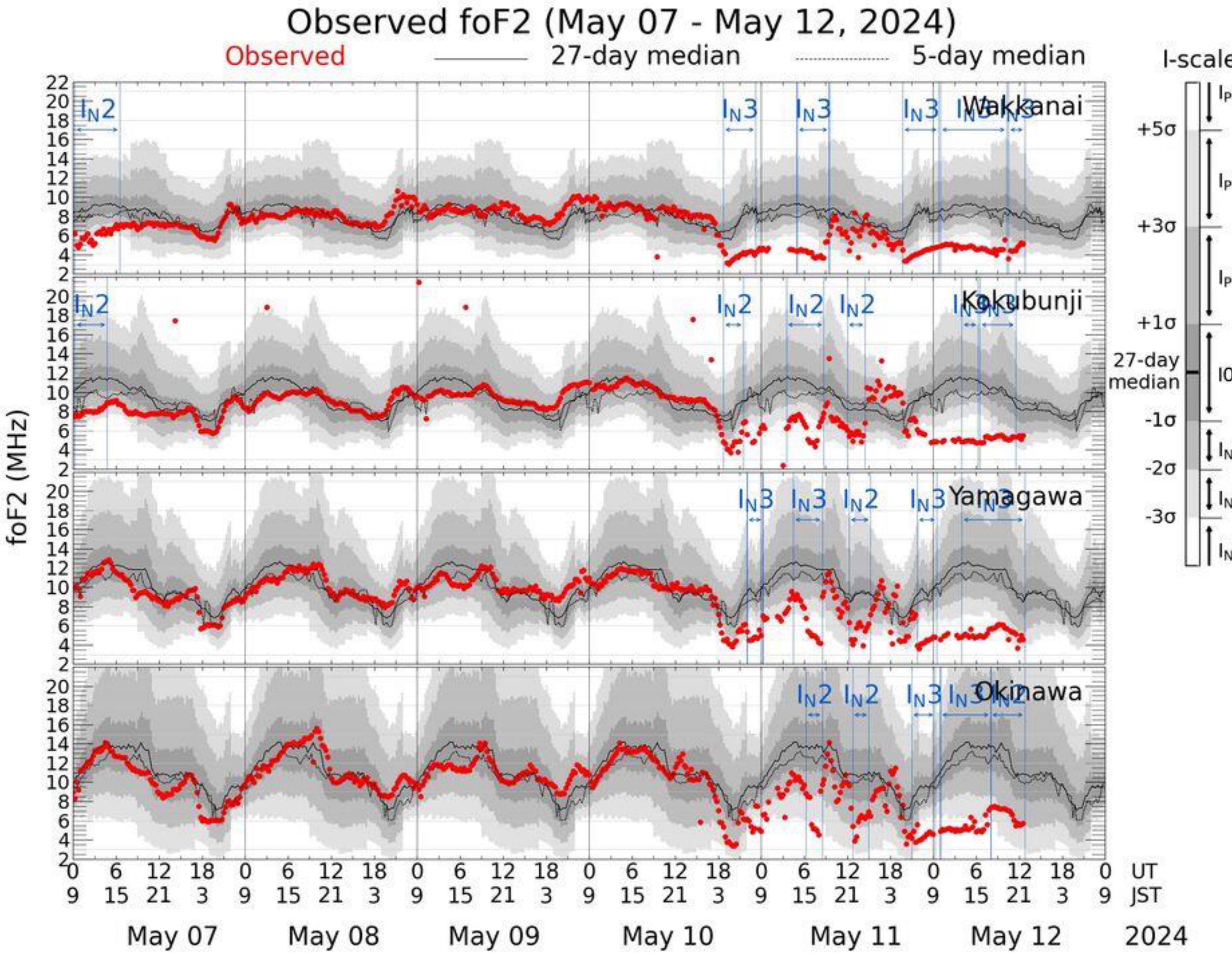

Ionospheric Monitoring and Prediction Center (IMPC by DLR), ESA SWESNET:

ROTI values enhanced after the X5 flare on May 11 (01:23 UTC)

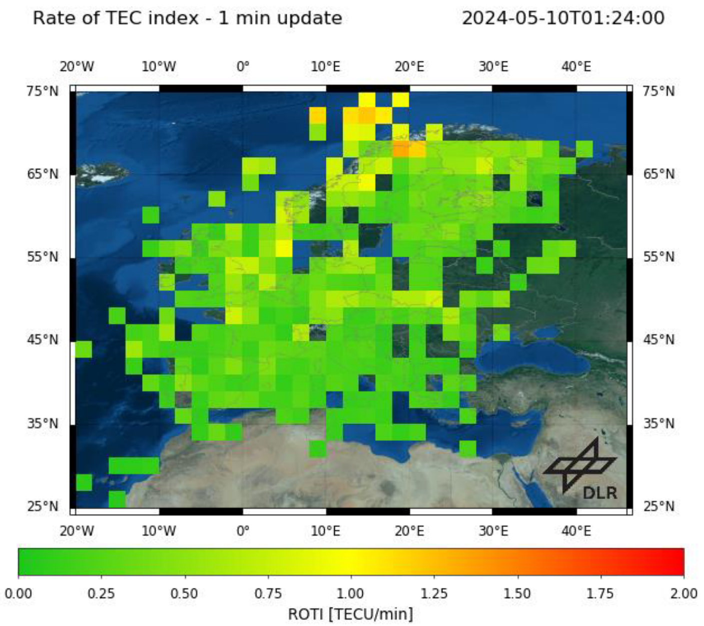

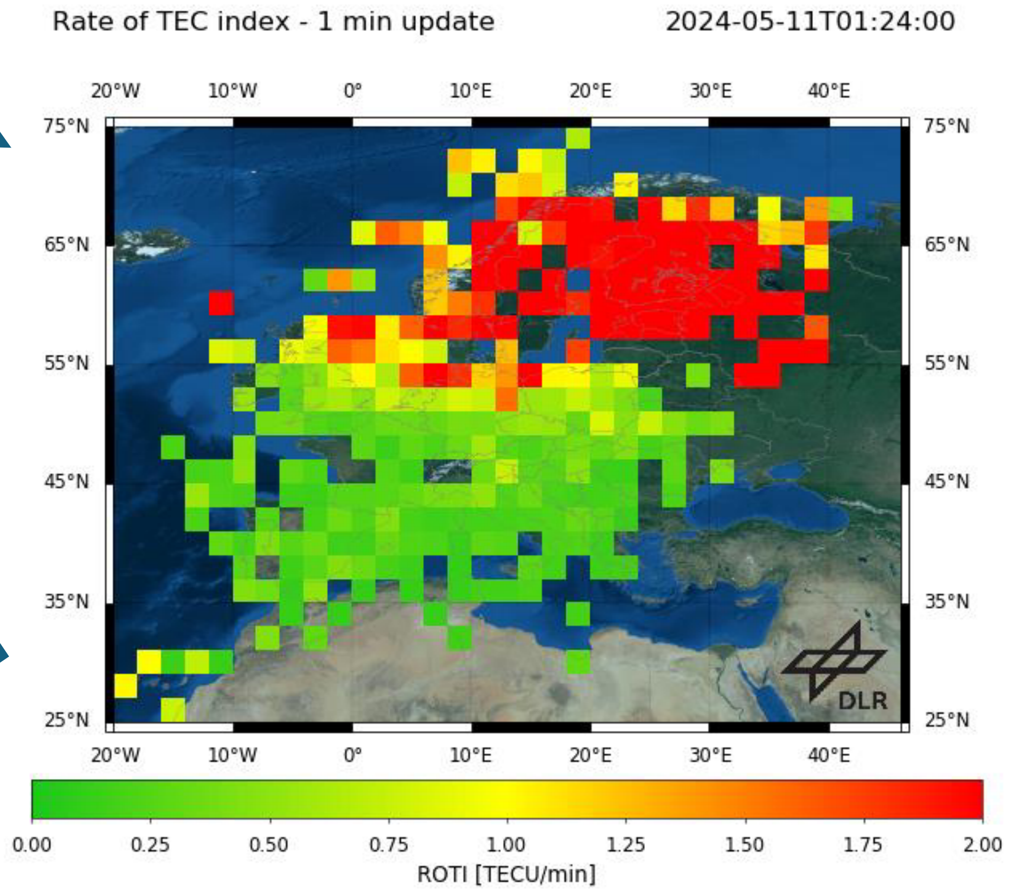

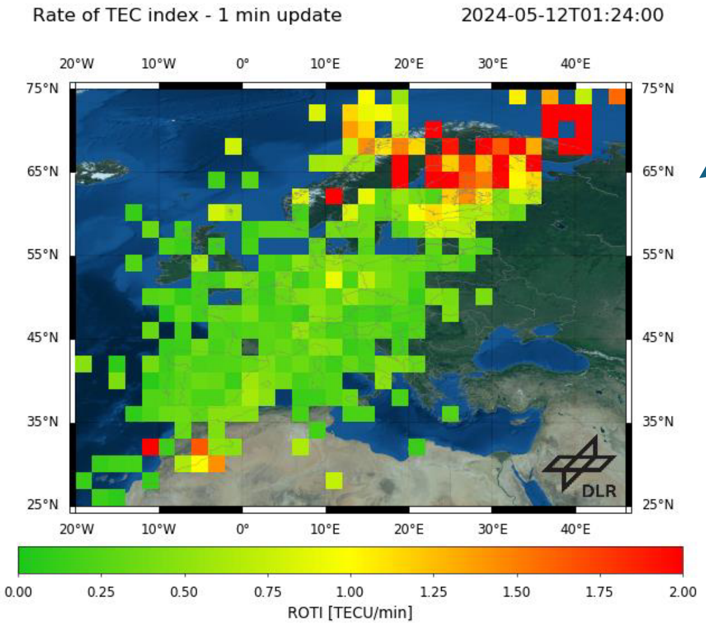

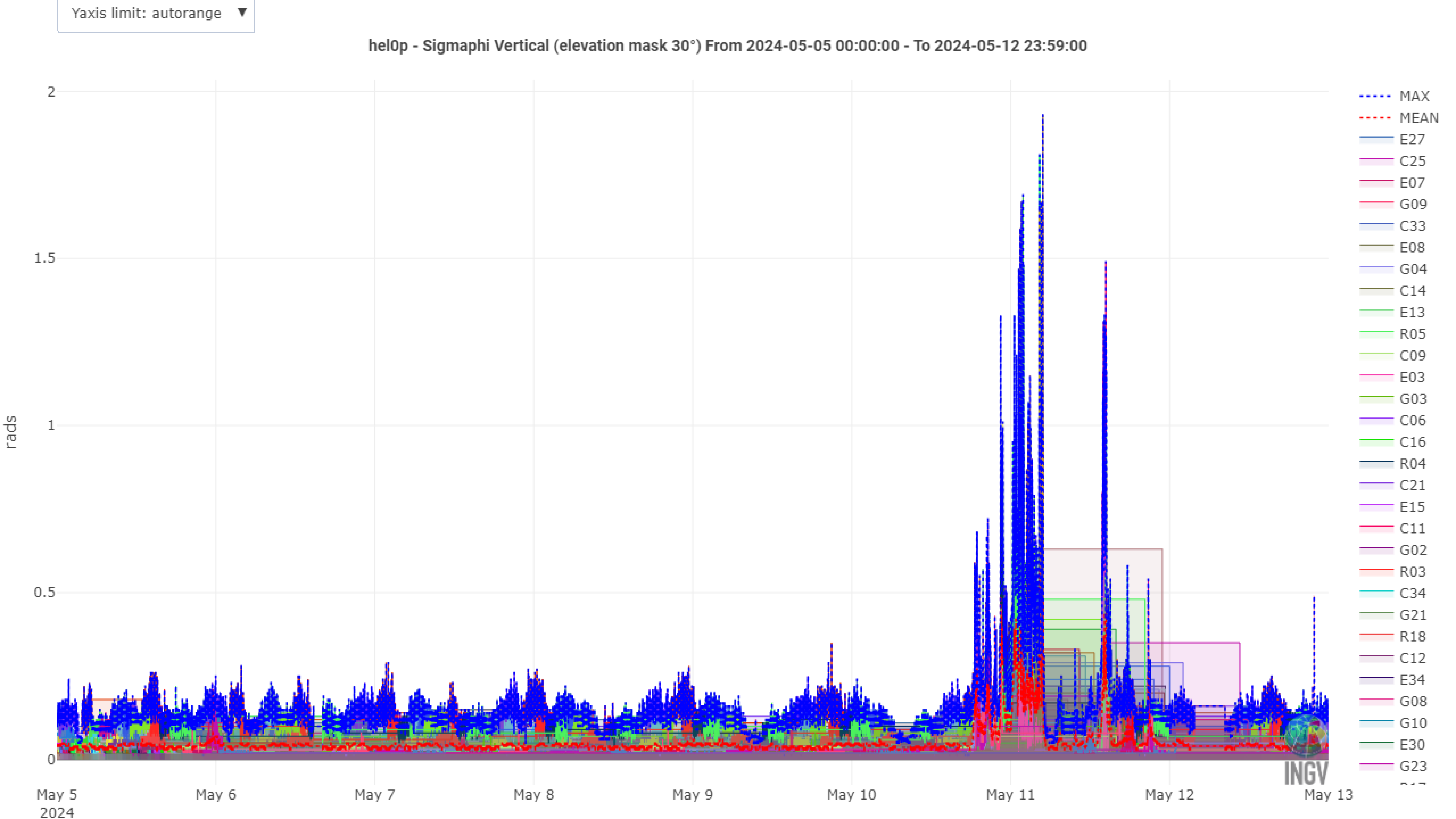

Yaxis limit: autorange
hel0p - Sigmaphi Vertical (elevation mask 30°) From 2024-05-05 00:00:00 - To 2024-05-12 23:59:00
rads
2
1.5
1
0.5
0
May 5
2024
May 6
May 7
May 8
May 9
May 10
May 11
May 12
May 13
MAX
MEAN
E27
C25
E07
G09
C33
E08
G04
C14
E13
R05
C09
E03
G03
C06
C16
R04
C21
E15
C11
G02
R03
C34
G21
R18
C12
E34
G08
G10
E30
G23
INGV

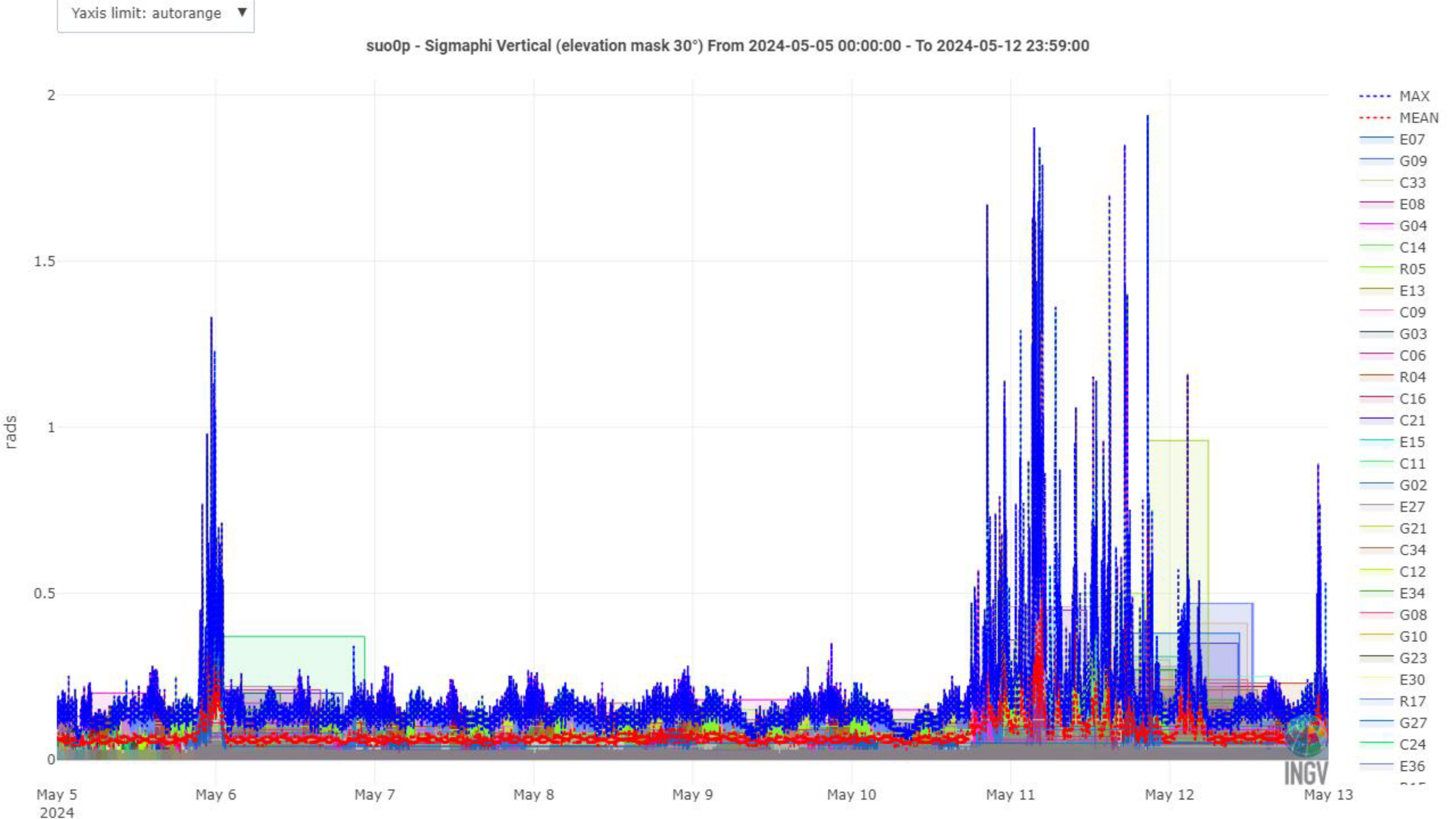

Yaxis limit: autorange
suo0p - Sigmaphi Vertical (elevation mask 30°) From 2024-05-05 00:00:00 - To 2024-05-12 23:59:00
rads
2
1.5
1
0.5
0
May 5
2024
May 6
May 7
May 8
May 9
May 10
May 11
May 12
May 13
MAX
MEAN
E07
G09
C33
E08
G04
C14
R05
E13
C09
G03
C06
R04
C16
C21
E15
C11
G02
E27
G21
C34
C12
E34
G08
G10
G23
E30
R17
G27
C24
E36
INGV

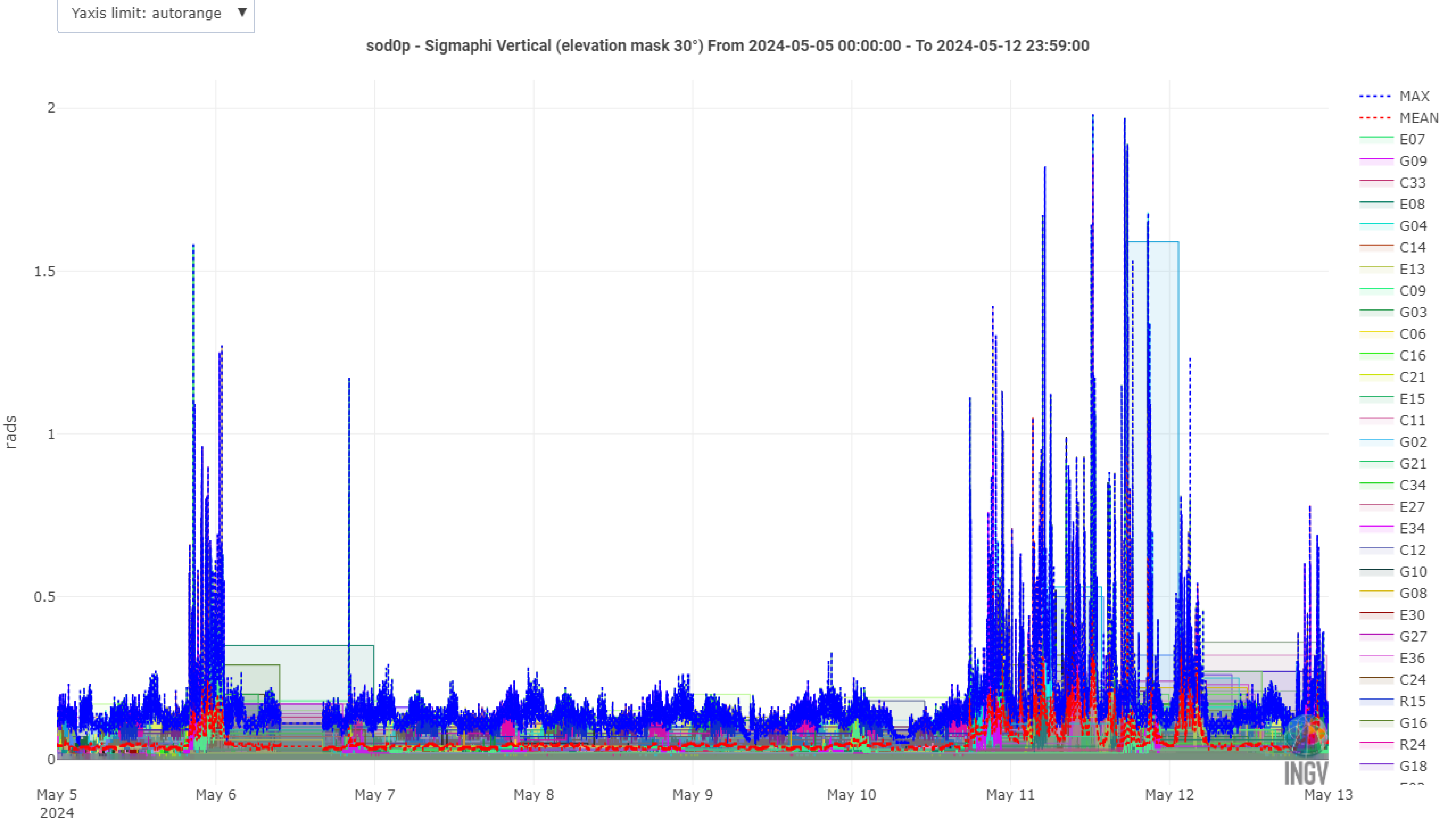

Yaxis limit: autorange
sod0p - Sigmaphi Vertical (elevation mask 30°) From 2024-05-05 00:00:00 - To 2024-05-12 23:59:00
rads
2
1.5
1
0.5
0
May 5
2024
May 6
May 7
May 8
May 9
May 10
May 11
May 12
May 13
MAX
MEAN
E07
G09
C33
E08
G04
C14
E13
C09
G03
C06
C16
C21
E15
C11
G02
G21
C34
E27
E34
C12
G10
G08
E30
G27
E36
C24
R15
G16
R24
G18
INGV

Summary

- Ionosphere impacts the propagation of radiowaves
  - Refraction with dispersion
  - Diffraction
  - Attenuation
  - Drops in Maximum Usable Frequency

- Critical parameters characterizing the impact
  - Frequency of the radio waves
  - Ionospheric electron density (controlled by interactions with magnetosphere and thermosphere)
  - Magnetic field & electron collisions with other particles

- Vulnerable systems
  - Applications based on ionospheric radio wave reflections in frequencies 30-300 MHz
  - Applications based on accurate positioning by Global Navigation Satellite Systems (GNSS)

- Dual role of GNSS
  - Impacted by ionospheric scintillation
  - Offers an opportunity to monitor ionospheric electron density by TEC maps and tomography

- Impacts can last from 0.5 hr to several days and are mostly difficult to forecast

Backup slides

More about the Appleton-Hartree equation

- Impact of ions can be neglected unless frequencies < 1kHz (ion gyrofrequency) are addressed
- Cold plasma approximation: v_p of signal >> plasma thermal speed = $\sqrt{2kBT/m}$
- No strong gradients in B (background magnetic field), i.e. no big changes in distance of signal wavelength $\lambda=2\pi/k$
- Derived independently also by German radio physicist Lassen (1927)

Some formulas behind Appleton-Hartree

The Maxwell equations:

$$\nabla \cdot \mathbf{D} = \rho_f, \tag{3.6}$$

$$\nabla \cdot \mathbf{B} = 0, \tag{3.7}$$

$$\nabla \times \mathbf{E} = -\frac{\partial \mathbf{B}}{\partial t}, \tag{3.8}$$

$$\nabla \times \mathbf{B} = \mu_0 \mathbf{j} + \frac{1}{c^2}\frac{\partial \mathbf{E}}{\partial t}. \tag{3.9}$$

In linear media, the fields $\mathbf{E}$ and $\mathbf{B}$ are related to $\mathbf{D}$ and $\mathbf{H}$ by the constitutive relations

$$\mathbf{D} = \varepsilon_0 \boldsymbol{\varepsilon}_r \cdot \mathbf{E}, \tag{3.10}$$

$$\mathbf{B} = \mu_0 \boldsymbol{\mu}_r \cdot \mathbf{H} \approx \mu_0 \mathbf{H}. \tag{3.11}$$

Assumed to be ~1

$$c^2 = \frac{1}{\varepsilon_0 \mu_0},$$

Accounting for the anisotropic properties of plasma

Excerpts from Fontell Diploma Thesis (2018)

Some formulas behind Appleton-Hartree

Fluid description of plasma; continuity and momentum equations:

particle species α:

$$\frac{\partial N_\alpha}{\partial t} + \nabla \cdot (N_\alpha \mathbf{u}_\alpha) = 0, \tag{3.1}$$

$$N_\alpha m_\alpha \frac{\partial \mathbf{u}_\alpha}{\partial t} + N_\alpha m_\alpha \mathbf{u}_\alpha \cdot \nabla \mathbf{u}_\alpha - N_\alpha q_\alpha (\mathbf{E} + \mathbf{u}_\alpha \times \mathbf{B}) + \nabla \cdot \boldsymbol{P}_\alpha = \boxed{m_\alpha \int \mathbf{v} \left(\frac{\partial f_\alpha}{\partial t} \right)_c d^3\mathbf{v}.} \tag{3.2}$$

For electrons:

$$\approx -m_e N_e \mathbf{u}_e \nu_{en}.$$

and

$$\mathbf{j} = \mathbf{j}_e = -eN_e \mathbf{u}_e.$$

Solving the inverse of the matrix in eqn. (3.24) gives Ohm's law

$$\mathbf{j} = \boldsymbol{\sigma} \cdot \mathbf{E},$$

where $\boldsymbol{\sigma}$ is the sought conductivity tensor

$$\boldsymbol{\sigma} = i\omega\varepsilon_0 \frac{X}{U^2 - Y^2} \begin{bmatrix} U & -iY & 0 \\ iY & U & 0 \\ 0 & 0 & \frac{U^2 - Y^2}{U} \end{bmatrix}.$$

Excerpts from Fontell Diploma Thesis (2018)

Some formulas behind Appleton-Hartree

$$\nabla \cdot \mathbf{D} = \rho_f, \tag{3.6}$$
$$\nabla \cdot \mathbf{B} = 0, \tag{3.7}$$
$$\nabla \times \mathbf{E} = -\frac{\partial \mathbf{B}}{\partial t}, \tag{3.8}$$
$$\nabla \times \mathbf{B} = \mu_0 \mathbf{j} + \frac{1}{c^2}\frac{\partial \mathbf{E}}{\partial t}. \tag{3.9}$$

In linear media, the fields **E** and **B** are related to **D** and **H** by the constitutive relations

$$\mathbf{D} = \varepsilon_0 \boldsymbol{\varepsilon}_r \cdot \mathbf{E}, \tag{3.10}$$
$$\mathbf{B} = \mu_0 \boldsymbol{\mu}_r \cdot \mathbf{H} \approx \mu_0 \mathbf{H}. \tag{3.11}$$

E and perturbations in **B** and N_e are assumed to be of the form:

$$g(\mathbf{r}, t) \propto e^{i(\mathbf{k}\cdot\mathbf{r} - \omega t)}$$

$$\frac{\partial}{\partial t} \rightarrow -i\omega, \tag{3.15}$$
$$\nabla \cdot \rightarrow i\mathbf{k}\cdot, \tag{3.16}$$
$$\nabla \times \rightarrow i\mathbf{k}\times \tag{3.17}$$

Goal: Derive an equation from which E can be solved

Excerpts from Fontell Diploma Thesis (2018)

Some formulas behind Appleton-Hartree

$$\nabla \cdot \mathbf{D} = \rho_f, \quad (3.6)$$
$$\nabla \cdot \mathbf{B} = 0, \quad (3.7)$$
$$\nabla \times \mathbf{E} = -\frac{\partial \mathbf{B}}{\partial t}, \quad (3.8)$$
$$\nabla \times \mathbf{B} = \mu_0 \mathbf{j} + \frac{1}{c^2}\frac{\partial \mathbf{E}}{\partial t}. \quad (3.9)$$

In linear media, the fields **E** and **B** are related to **D** and **H** by the constitutive relations

$$\mathbf{D} = \varepsilon_0 \boldsymbol{\varepsilon}_r \cdot \mathbf{E}, \quad (3.10)$$
$$\mathbf{B} = \mu_0 \boldsymbol{\mu}_r \cdot \mathbf{H} \approx \mu_0 \mathbf{H}. \quad (3.11)$$

$$\Rightarrow \quad \frac{c^2}{\omega^2}\mathbf{k} \times (\mathbf{k} \times \mathbf{E}) + \boldsymbol{\varepsilon}_r \cdot \mathbf{E} = \mathbf{0},$$

where

$$\boldsymbol{\varepsilon}_r \equiv \boldsymbol{\mathcal{I}} + \frac{i}{\omega \varepsilon_0}\boldsymbol{\sigma}$$

Now, finally the refraction index is introduced to the formulation: $\mathbf{k} = \frac{\mathbf{n}\omega}{c}$

$$\frac{c^2}{\omega^2}\mathbf{k} \times (\mathbf{k} \times \mathbf{E}) + \boldsymbol{\varepsilon}_r \cdot \mathbf{E} = \mathbf{0}, \quad \Rightarrow \quad \mathbf{n}(\mathbf{n} \cdot \mathbf{E}) - n^2\mathbf{E} + \boldsymbol{\varepsilon}_r \cdot \mathbf{E} = \mathbf{0}. \quad \Rightarrow \quad \mathbf{M} \cdot \mathbf{E} = \mathbf{0}.$$

$$\mathbf{a} \times (\mathbf{b} \times \mathbf{c}) = \mathbf{b}(\mathbf{a} \cdot \mathbf{c}) - \mathbf{c}(\mathbf{a} \cdot \mathbf{b})$$

Matrix formulation

Solution for **E** can be found only if det(M)=0 $\Rightarrow$ Equation for n whose solution is the Appleton-Hartree eq.

Excerpts from Fontell Diploma Thesis (2018)